

ABSTRACT

ZHAO, RUNZHI. Three Chapters on Financial Econometrics. (Under the direction of Denis Pelletier).

This dissertation centers on modeling the volatility of stock returns and applying such models to stock markets.

In Chapter 1, we let some of the parameters be time-varying and extend the Realized GARCH model to the Time-Varying Parameter Realized GARCH (TVP-RGARCH) model. We assume that the time-varying parameters follow the AR(1) process and use the Efficient Importance Sampling (EIS) method to estimate the model. Our simulation study finds that such a model captures the trend of the time-varying parameters very well, either for in-sample or out-of-sample observations, and the forecasting performance is slightly better than the benchmark Realized GARCH model. The empirical study shows that for some of the stock indices, the parameters should be regarded as time-varying.

In Chapter 2, we incorporate the VIX index into the Realized GARCH model and extend the model to the Realized GARCH-VIX model. In our model, we assume that the conditional variance has two components: the variance driven by realized volatility and the variance driven by the VIX index. The empirical analysis suggests that our model has a better forecasting performance than the benchmark Realized GARCH model. Further rolling window analysis finds that our model is better in volatility forecasting than the benchmark Realized GARCH model in most of the windows, and for some windows, it is statistically better at the significance of 10%.

In Chapter 3, we study the spillover effect of return and volatility between global stock markets by using the connectedness network approach. We include a global endogenous shock - the US monetary policy shock to the connectedness network to study the interaction between global stock markets and such endogenous shock. In our analysis, we find that: first, the volatility system has more interactions than the return system; second, in the 20-year whole

sample, the US monetary shock plays a minor role in the global stock market connectedness; third, the US monetary policy plays an important role in the period of the 2008 financial crisis and after the outbreak of COVID, and the effect of the shock is utterly contrary to each other during the two different special periods.

© Copyright 2023 by Runzhi Zhao

All Rights Reserved

Three Chapters on Financial Econometrics

by
Runzhi Zhao

A dissertation submitted to the Graduate Faculty of
North Carolina State University
in partial fulfillment of the
requirements for the Degree of
Doctor of Philosophy

Economics

Raleigh, North Carolina
2023

APPROVED BY:

Zheng Li

Ilze Kalnina

Mehmet Caner

Denis Pelletier
Chair of Advisory Committee

BIOGRAPHY

Runzhi Zhao was born in a small town Heqiao in Jiangsu Province of China. He got a Bachelor's Degree of Science in Astronomy from Nanjing University, and then he finished a Master's Degree in Economics in Nanjing University. After that, began on August 2018, he traveled to the US and started working on the Ph.D. program in Economics and finally focused on the study of financial econometrics.

TABLE OF CONTENTS

List of Tables	v
List of Figures	vi
Chapter 1 Time-Varying Parameter Realized GARCH Model	1
1.1 Introduction	1
1.2 Realized Volatility: a Short Review	3
1.3 Model Setting	5
1.4 Estimation: MC-EIS Method	8
1.5 Simulation Study	13
1.5.1 Estimation	13
1.5.2 Forecast Performance Evaluation	15
1.6 Empirical Analysis	16
1.6.1 Data Description	16
1.6.2 Empirical Estimation Results	18
1.6.3 Forecasting Performance Comparison	19
1.7 Conclusion	20
Chapter 2 Does VIX Have Additional Information to Realized Volatility? Evidence from S&P 500 and VIX Index	22
2.1 Introduction	22
2.2 VIX Index: a Review	25
2.3 Model Specification	27
2.4 Model Estimation	29
2.4.1 Likelihood of Realized GARCH Model	30
2.4.2 Likelihood of Realized GARCH-VIX Model	30
2.5 Data and Empirical Results	31
2.5.1 Data Description	31
2.5.2 Parameter Estimates	31
2.5.3 Forecasting Performance	32
2.5.4 Estimation and Forecasting in Rolling Windows	34
2.6 Conclusion	42
Chapter 3 US Monetary Shock and Spillover Effect in Stock Market between Countries 43	43
3.1 Introduction	43
3.2 Federal Funds Rate and the US Monetary Shock	46
3.3 Model and Methodology	47
3.4 Empirical Results	50
3.4.1 Return System Spillover	51
3.4.2 Volatility System Spillover	56
3.4.3 Rolling Window Analysis	59
3.4.4 Spillover During the 2008 Financial Crisis	62
3.4.5 Spillover after the COVID-19 Outbreak	68

3.5	Robustness Test	72
3.6	Conclusion	73
References	75
APPENDICES	80
Appendix A	Tables and Figures	81
Appendix B	Calculation of VIX	84
Appendix C	Diebold-Mariano Test.....	86

LIST OF TABLES

Table 1.1	EIS Estimation of TVP Realized GARCH Model	15
Table 1.2	Forecasting Performance	16
Table 1.3	EIS Estimation of TVP Realized GARCH Model	19
Table 1.4	Estimates of benchmark Realized GARCH Model	20
Table 1.5	Out-of-Sample MSE Comparison for All Stock Indices	20
Table 2.1	Descriptive Statistics	32
Table 2.2	Estimation Results	32
Table 2.3	In-Sample Forecasting Performance	33
Table 2.4	Out-of-Sample Forecasting Performance in Rolling Windows	37
Table 3.1	Whole Sample Return Connectedness without Federal Funds Rate	54
Table 3.2	Whole Sample Return Connectedness with Federal Funds Rate	55
Table 3.3	Whole Sample Volatility Connectedness without Federal Funds Rate	56
Table 3.4	Whole Sample Volatility Connectedness with Federal Funds Rate	56
Table 3.5	Return Connectedness without FFR during 2008 Financial Crisis	65
Table 3.6	Return Connectedness with FFR during 2008 Financial Crisis	65
Table 3.7	Volatility Connectedness without FFR during 2008 Financial Crisis	66
Table 3.8	Volatility Connectedness with FFR during 2008 Financial Crisis	66
Table 3.9	Return Connectedness without FFR after COVID Outbreak	70
Table 3.10	Return Connectedness with FFR after COVID Outbreak	70
Table 3.11	Volatility Connectedness without FFR after COVID Outbreak	72
Table 3.12	Volatility Connectedness with FFR after COVID Outbreak	72
Table A.1	Descriptive statistics for daily returns	81
Table A.2	Descriptive statistics for 5-min realized volatility	82

LIST OF FIGURES

Figure 1.1	In-Sample ω_t	16
Figure 1.2	Out-of-Sample ω_t	17
Figure 2.1	VIX vs. Realized Volatility	27
Figure 2.2	Normalized VIX vs. Realized Volatility	28
Figure 2.3	In-Sample Forecasting Performance of Realized GARCH-VIX Model	33
Figure 2.4	Out-of-Sample Forecasting Performance of Realized GARCH-VIX Model	34
Figure 2.5	Time Varying κ	35
Figure 2.6	MSE Difference for Rolling Windows	36
Figure 3.1	Weekly Return Series	51
Figure 3.2	Weekly Volatility Series	52
Figure 3.3	Weekly Federal Funds Rate Series	53
Figure 3.4	Dynamics of Total Spillover in Return System	60
Figure 3.5	Dynamics of Total Spillover in Volatility System	61
Figure 3.6	Spillover to the Return System	63
Figure 3.7	Spillover to the Volatility System	64
Figure 3.8	Dynamic Total Spillovers for Various Rolling Windows in the Return System	73
Figure 3.9	Dynamic Total Spillovers for Various Rolling Windows in the Volatility System	74
Figure A.1	The Daily Returns of 6 Stock Indices	82
Figure A.2	The 5-Min Realized Volatility of 6 Stock Indices	83

CHAPTER

1

TIME-VARYING PARAMETER REALIZED GARCH MODEL

1.1 Introduction

High-frequency data is getting easier to access in recent years. Volatility, which was a latent variable in traditional econometric models, like Generalized AutoRegressive Conditional Heteroskedasticity (GARCH) model (see Bollerslev (1986)) and stochastic volatility model (see Taylor (2007)), now becomes "observable" and can be directly modelled. A number of realized measures of volatility are modelled and constructed from high-frequency data (see Anderson and Bollerslev (1998), Anderson et al. (2003), Meddahi (2002), Aït-Sahalia et al. (2005), Bandi and Russell (2006), Hansen and Lunde (2006)).

Some researchers have incorporated realized volatility into the traditional GARCH model. Engle (2002) estimated a GARCH model including realized volatility, which is known as GARCH-X model thereafter (see also Forsberg and T (2002)). This model captures the dynamics of conditional variance of returns using lagged realized volatility, but it does not relate the realized volatility with returns in the future. Engle and Gallo (2006) made a further step into this model by combining three realized measures of volatility in the multiplicative error model (MEM), as suggested by Engle (2002). Shephard and Sheppard (2010) and Noureldin D and Sheppard (2012) introduced a HEAVY model base on the structure of MEM framework. Both MEM and HEAVY models operate with multiple latent volatility processes. They are recognized as a "complete" model because a measurement equation is built up for multi-step forecasting of the future daily returns in each of them.

Hansen et al. (2011) introduced the realized GARCH model which directly links realized volatility to the conditional variance of daily returns and includes a term that captures the leverage effect. This model is easy to estimate since it includes the realized volatility in the GARCH equation, and proved to be more efficient in short-term forecasting, typically within 7 days. A number of extensions of realized GARCH model have been developed based on the benchmark of Hansen et al. (2011). For example, Hansen and Huang (2016) introduced the realized exponential GARCH model, which uses the logarithmic form of conditional variance of daily returns and realized volatility in both of the GARCH equation and the measurement equation; Gerlach et al. (2020) allowed the parameters in the GARCH equation to be time-variable and as a function of an estimator of the asymptotic variance of the realized measure, and tackled the attenuation bias issue of the Hansen et al. (2011) benchmark with this time-varying coefficient realized GARCH model.

This chapter develops a new approach to construct a time-varying parameter Realized GARCH model based on the Hansen et al. (2011) benchmark. Unlike Gerlach et al. (2020), here we assume that the parameters in the GARCH equation follow a stationary AR(1) process, and then use the efficient importance sampling (EIS) method to estimate the parameters.

The rest of this paper is organized as follows: Section 2 reviews the basic theoretical framework and the computation of realized measures of volatility; Section 3 introduces the framework of our model; Section 4 reviews the EIS method to get an accurate numerical approximation of the log-likelihood of our model; Section 5 presents a simulation study; Section 6 discusses empirical findings and compares our results with other models; Section 7 concludes this article and proposes potential further extensions.

1.2 Realized Volatility: a Short Review

In recent years, the availability of high-frequency financial market data has enabled researchers to build reliable measures of the latent daily volatility, based on the use of intra-daily returns. In the econometric and financial literature, these are widely known as realized volatility measures. The theoretical background of these measures is given by a dynamic specification of the price process in continuous time. Formally, let the logarithmic price p_t of a financial asset be determined by the stochastic differential process

$$d_{p_t} = \mu_t dt + \sigma_t dW_t, \quad 0 \leq t \leq T, \quad (1.1)$$

where μ_t and σ_t are the drift and instantaneous volatility processes, respectively, whilst W_t is a standard Brownian motion; σ_t is assumed to be independent of W_t . Under the assumption of a frictionless market, the logarithmic price p_t follows a semi-martingale process. In that case, given a sequence of partitions $t - 1 = \tau_0 \leq \tau_1 \leq \dots \leq \tau_M = t$, the Quadratic Variation (QV) of log-returns $r_t = p_t - p_{t-1}$, given by

$$QV_t = p \lim_{M \rightarrow \infty} \sum_{j=0}^{M-1} (p_{\tau_{j+1}} - p_{\tau_j})^2,$$

coincides with the Integrated Variance (IV)

$$IV_t = \int_{t-1}^t \sigma_s^2 ds. \quad (1.2)$$

In the absence of microstructure noise and measurement errors, Barndorff-Nielsen and Shephard (2002) show that IV is consistently estimated by Realized Volatility (RV)

$$RV_t = \sum_{i=1}^M r_{t,i}^2, \quad (1.3)$$

where

$$r_{t,i} = p_{t-1+i\Delta} - p_{t-1+(i-1)\Delta}$$

is the i -th Δ -period intraday return, $M = 1/\Delta$. Although IV and the conditional variance of returns do not coincide, there is a precise relationship between these two quantities: under standard integrability conditions (Andersen et al. (2001)) it can be shown that

$$E(IV_t | \mathcal{F}_{t-1}) = var(r_t | \mathcal{F}_{t-1}), \quad (1.4)$$

where \mathcal{F}_{t-1} denotes the information set at time $(t-1)$. In other words, the optimal forecast of IV can be interpreted as the conditional variance of returns and the difference between these two quantities is given by a zero mean error. As mentioned above, Barndorff-Nielsen and Shephard (2002) showed that RV consistently estimates the true latent volatility, as $\Delta \rightarrow 0$. They also find that, conditional on the realization of IV_t , the asymptotic distribution of RV_t is Gaussian,

$$\frac{\sqrt{M}(RV_t - IV_t)}{\sqrt{2IQ_t}} \xrightarrow{d} N(0, 1), \quad (1.5)$$

where $IQ_t = \int_{t-1}^t \sigma_s^4 ds$ is the Integrated Quarticity (IQ). This, in turn, can be consistently estimated as

$$RQ_t = \frac{M}{3} \sum_{i=1}^M r_{t,i}^4. \quad (1.6)$$

Replacing IQ_t by RQ_t in Eq. (1.5) still gives

$$\frac{\sqrt{M}(RV_t - IV_t)}{\sqrt{2RQ_t}} \xrightarrow{d} N(0, 1). \quad (1.7)$$

In financial modeling, the use of $\mathbf{log}(RV_t)$ is often preferred to the “plain” RV_t estimator, due to its favorable finite sample properties (see Corsi et al. (2008), among others). The approximate asymptotic distribution of $\mathbf{log}(RV_t)$ can be shown to be

$$\frac{\sqrt{M}(\mathbf{log}(RV_t) - \mathbf{log}(IV_t))}{\sqrt{\frac{2RQ_t}{RV_t^2}}} \xrightarrow{d} N(0, 1). \quad (1.8)$$

Furthermore, Corsi et al. (2008) provide empirical evidence that, in a HAR model, choosing the logarithmic realized variance as a dependent variable and allowing for time-varying volatility of realized volatility leads to substantial improvements in fit and forecasting performance.

1.3 Model Setting

Following Hansen et al. (2011) and Hansen and Huang (2016), the realized exponential GARCH(1,1) model is represented by the following equations:

$$r_t = \sqrt{h_t} z_t \quad (1.9)$$

$$\mathbf{log} h_t = \omega + \beta \mathbf{log} h_{t-1} + \gamma \mathbf{log} x_{t-1} \quad (1.10)$$

$$\mathbf{log} x_t = \xi + \varphi \mathbf{log} h_t + \tau(z_t) + u_t \quad (1.11)$$

where r_t denotes the daily returns with $\mathbb{E}[r_t | \mathcal{F}_{t-1}] = 0$, $h_t = \mathbb{E}[r_t^2 | \mathcal{F}_{t-1}]$ (\mathcal{F}_{t-1} is the information set up to time $t - 1$) is the conditional variance of daily returns, x_t denotes a realized measure of volatility. The random errors z_t and u_t are assumed to be independent, with $z_t \sim N(0, 1)$

and $u_t \sim N(0, \sigma_u^2)$. Finally, $\tau(z_t) = \tau_1 z_t + \tau_2 (z_t - 1)^2$ denotes the leverage effect, which captures the dependence between returns and future volatility. Eq. (1.9), (1.10) and (1.11) in the realized GARCH model, according to Hansen et al. (2011), are referred as *return equation*, *GARCH equation* and *measurement equation*, respectively.

In this paper, we extend this model by letting the parameters of the GARCH equation be time-variable according to an AR(1) process, i.e., Eq. (1.10) becomes:

$$\mathbf{log}h_t = \omega_t + \beta_t \mathbf{log}h_{t-1} + \gamma_t \mathbf{log}x_{t-1} \quad (1.12)$$

and the time-varying parameters $(\omega_t, \beta_t, \gamma_t)'$ follow the AR(1) process defined as:

$$\begin{pmatrix} \omega_t \\ \beta_t \\ \gamma_t \end{pmatrix} = \begin{pmatrix} \bar{\omega} \\ \bar{\beta} \\ \bar{\gamma} \end{pmatrix} + \mathbf{A} \begin{pmatrix} \omega_{t-1} \\ \beta_{t-1} \\ \gamma_{t-1} \end{pmatrix} + \epsilon_t \quad (1.13)$$

where \mathbf{A} is a 3×3 matrix whose absolute values of eigenvalues are less than 1 (if the eigenvalues are complex numbers, then the modules of the eigenvalues should be less than 1), $\epsilon_t \sim \mathbf{N}(0, \Omega)$ where Ω is a 3×3 covariance matrix.

To improve the accuracy of the estimation and reduce the variance of the parameters, we further assume that all the time-varying parameters in the GARCH equation are driven by a single time series latent variables λ_t . The relationship between the time-varying parameters and the time-series latent variables is defined as:

$$\begin{pmatrix} \omega_t \\ \beta_t \\ \gamma_t \end{pmatrix} = \begin{pmatrix} \omega_0 \\ \beta_0 \\ \gamma_0 \end{pmatrix} + D\lambda_t \quad (1.14)$$

and

$$\lambda_t = \delta\lambda_{t-1} + \nu\eta_t, \quad (1.15)$$

where $(\omega_0, \beta_0, \gamma_0)'$ denotes the unconditional mean of the time-varying parameters, $D = (d_1, d_2, d_3)'$ represents the parameter loadings, δ and ν are the parameters of the AR(1) process, and $\eta_t \sim N(0, 1)$. Combined with Eq. (1.14) and (1.15), Eq. (1.13) can be re-written as:

$$\begin{pmatrix} \omega_t \\ \beta_t \\ \gamma_t \end{pmatrix} = (1 - \delta) \begin{pmatrix} \omega_0 \\ \beta_0 \\ \gamma_0 \end{pmatrix} + A \begin{pmatrix} \omega_{t-1} \\ \beta_{t-1} \\ \gamma_{t-1} \end{pmatrix} + \epsilon_t$$

where where $A = \delta I$ and $\epsilon \sim N(0, \nu^2 D D')$.

Then our model could be written as:

$$r_t = \sqrt{h_t} z_t \quad (1.16)$$

$$\mathbf{log} h_t = \omega_t + \beta_t \mathbf{log} h_{t-1} + \gamma_t \mathbf{log} x_{t-1} \quad (1.17)$$

$$\mathbf{log} x_t = \xi + \varphi \mathbf{log} h_t + \tau(z_t) + u_t \quad (1.18)$$

where the time-varying parameters $(\omega_t, \beta_t, \gamma_t)'$ satisfy Eq. (1.14) and (1.15). We refer to this model as the time-varying parameter Realized GARCH model (TVP-RGARCH model).

We note that the parameter loadings $D = (d_1, d_2, d_3)'$ determines only the variances of the time-varying parameters. However, the variances could also be changed by the value of ν . Thus here we have 4 parameters determining 3 variances. In order to achieve identification of this model, we impose a restriction on ν such that $\nu = 0.2$. (In our empirical analysis, we make the parameter ν relatively small so that the values of loading parameters D are not closed to zero).

The likelihood function of the TVP-RGARCH(1,1) model is given by:

$$\begin{aligned} L(r, x; \theta) &= \int \prod_{t=1}^T f(r_t, x_t, \lambda_t | r_{t-1}, x_{t-1}, \Lambda_{t-1}; \theta) d\Lambda \\ &= \int \prod_{t=1}^T p(r_t, x_t | r_{t-1}, x_{t-1}, \Lambda_t; \theta) q(\lambda_t | \Lambda_{t-1}; \theta) d\Lambda \end{aligned} \quad (1.19)$$

where $\Lambda = \lambda_{t=1}^T$, and $\Lambda_{t-1} = \lambda_{\tau=1}^{t-1}$.

The distribution function p in Eq. (1.19) represents the conditional density of $\{r_t, x_t\}$ conditioning on the density of λ_t given $(r_{t-1}, x_{t-1}, \Lambda_{t-1})$, and q denotes the conditional distribution of λ_t given Λ_{t-1} . In order to complete the statistical specification, we define $q(\lambda_1|\Lambda_0; \theta) = q(\lambda_1; \theta)$ as the unconditional distribution of λ_1 under the AR(1) process given by Eq. (1.14). Under our TVP-RGARCH model, the relevant distribution functions are given by:

$$p(r_t, x_t | r_{t-1}, x_{t-1}, \Lambda_t; \theta) = \frac{1}{2\pi\sqrt{h_t\sigma_u^2}} \mathbf{exp} \left[- \left(\frac{r_t^2}{2h_t} + \frac{u_t^2}{2\sigma_u^2} \right) \right] \quad (1.20)$$

and

$$q(\lambda_t | \Lambda_{t-1}; \theta) = \begin{cases} \frac{1}{\sqrt{2\pi\gamma^2/(1-\delta^2)}} \mathbf{exp}\{-\frac{1-\delta^2}{2\gamma^2} \lambda_t^2\}, & t = 1 \\ \frac{1}{\sqrt{2\pi\gamma^2}} \mathbf{exp}\{-\frac{1}{2\gamma^2}(\lambda_t - \delta\lambda_{t-1})\}, & t : 2 \rightarrow T \end{cases} \quad (1.21)$$

Then the log-likelihood function could be written as:

$$\ell(r, x; \theta) = \mathbf{log}L(r, x; \theta) \quad (1.22)$$

We estimate this model by maximizing the likelihood function with respect to those parameters.

1.4 Estimation: MC-EIS Method

It is hard to get the likelihood function L directly using Eq. (1.19) because the multiple integrals do not have a closed-form expression, so here we develop an accurate numerical approximation \tilde{L}_N of the likelihood function L with the efficient importance sampling (EIS) method.

Importance sampling method was first introduced by Kloek and van Dijk (1978), and it is aimed at gaining the statistical properties of a particular distribution while only having samples generated from a different distribution than the distribution of interest. The basic idea of this method is to draw N trajectories of the time-varying parameters $\{\lambda_1^{(i)}, \dots, \lambda_T^{(i)} : i = 1 \rightarrow N\}$ from certain distributions (e.g. the q distribution, referred as natural sampler) to get the Monte Carlo (MC) estimation of $L(r, x; \theta)$ from Eq. (1.19), replacing the integrals by a sample average over

the N trajectories.

However, it has shown that the direct MC estimation of likelihood $L(r, x; \theta)$ based on the natural sampler is inefficient, i.e, it cannot obtain an accurate MC numerical approximation \tilde{L}_N close to the true $L(r, x; \theta)$. The reason lies in the fact that simulated λ_t trajectories from the natural sampler typically do not bear any resemblance to the actual unobserved λ_t sequence under which the observed process r_t is generated. In other words, the implicit posterior density of Λ is much tighter than its prior (the natural sampler), whence potential efficiency gains are enormous.

In order to improve the efficiency of importance sampling MC estimate of $L(r, x; \theta)$, we apply the EIS method introduced by Liesenfeld and Richard (2006) and Richard and Zhang (2007) to provide a close approximation to the posterior of the implicit time-varying parameters Λ . Let $\{m(\lambda_t|\Lambda_{t-1}; a_t)\}_{t=1}^T$ be the sequence of auxiliary importance samplers with auxiliary parameters a_t to replace the natural sampler. Then for any given choice of the auxiliary parameters a_t , the likelihood function given by Eq. (1.19) could be rewritten as:

$$\begin{aligned} L(r, x; \theta) &= \int \prod_{t=1}^T f(r_t, x_t, \lambda_t | r_{t-1}, x_{t-1}, \Lambda_{t-1}; \theta) d\Lambda \\ &= \int \prod_{t=1}^T \frac{f(r_t, x_t, \lambda_t | r_{t-1}, x_{t-1}, \Lambda_{t-1}; \theta)}{m(\lambda_t | \Lambda_{t-1}; a_t)} m(\lambda_t | \Lambda_{t-1}; a_t) d\Lambda \end{aligned} \quad (1.23)$$

and the corresponding MC-EIS estimate of likelihood is given by:

$$\tilde{L}_N(r, x; \theta) = \frac{1}{N} \sum_{i=1}^N \left(\prod_{t=1}^T \frac{f(r_t, x_t, \lambda_t^{(i)} | r_{t-1}, x_{t-1}, \Lambda_{t-1}^{(i)}; \theta)}{m(\lambda_t^{(i)} | \Lambda_{t-1}^{(i)}; a_t)} \right) \quad (1.24)$$

where $\{\lambda_1^{(i)}, \dots, \lambda_T^{(i)} : i = 1 \rightarrow N\}$ are N independent trajectories drawn from the sequence of importance sampling densities m .

Natural choices for the importance samplers drawn from m are specified as parametric extensions of the natural sampler of density q . For the TVP-RGARCH model here, this indicates that the distribution m is a Gaussian density for $\lambda_t | \Lambda_{t-1}$. The goal of EIS method is to obtain

the optimized choice of a_t minimizing the MC estimate variance of the MC estimate likelihood given by Eq. (1.24). This requires that $\prod_t m_t$ be as close as possible to being proportional to $\prod_t f_t$. Accordingly, EIS approximations involve density kernels instead of density. In particular, we generate the auxiliary density m from density kernel $k(\lambda_t, \Lambda_{t-1}; a_t)$ satisfying:

$$m(\lambda_t | \Lambda_{t-1}; a_t) = \frac{k(\lambda_t, \Lambda_{t-1}; a_t)}{\chi(\Lambda_{t-1}; a_t)}, \quad \text{where} \quad \chi(\Lambda_{t-1}; a_t) = \int k(\lambda_t, \Lambda_{t-1}; a_t) d\lambda_t \quad (1.25)$$

Note that the integrating constant χ_t does not depend on λ_t , and χ_t could be backward transferred to the subproblem of the previous time period $t-1$ containing λ_{t-1} . Therefore, in order to obtain approximations of $f_t \chi_{t+1}$ by k_t , the sequential implementation of EIS requires solving a back-recursive sequence of auxiliary low-dimensional least squares problems of the form:

$$(\hat{c}_t, \hat{a}_t) = \underset{c_t, a_t}{\operatorname{argmin}} \sum_{i=1}^N \{ \log p(r_t, x_t | r_{t-1}, x_{t-1}, \check{\Lambda}_t^{(i)}; \theta) + \log q(\check{\lambda}_t^{(i)} | \check{\Lambda}_{t-1}^{(i)}; \theta) + \log \chi(\check{\Lambda}_t^{(i)}; \hat{a}_{t+1}) - c_t - \log k(\check{\lambda}_t^{(i)}, \check{\Lambda}_{t-1}^{(i)}; a_t) \}^2 \quad (1.26)$$

for $t : T \rightarrow 1$, with $\chi(\lambda_{T+1}, \cdot) = 1$. The N independent trajectories $\{\check{\lambda}_1^{(i)}, \dots, \check{\lambda}_T^{(i)} : i = 1 \rightarrow N\}$ are drawn from the sequence of q distributions and c_t 's are constants to be jointly estimated with a_t 's. In order to obtain maximally efficient EIS samplers, a small number of iterations of the EIS algorithm is required, where the initial samplers drawn from q are replaced by importance samplers with parameters estimated from the last stage, until the convergence of the a_t 's is reached. Note that if the importance sampler m_t is chosen within the exponential family of distributions, $\log k_t$ can be expressed as a linear function of a_t . This produces a significant simplification in that the optimization problem (1.26) becomes a linear least squares problem, which keeps the cost of computation down relative to corresponding nonlinear problems. The final MC-EIS estimate of the likelihood is obtained by substituting $\{\hat{a}_t\}_{t=1}^T$ for $\{a_t\}_{t=1}^T$ in Eq. (1.24), and the ML-ELS estimates of θ are obtained by maximizing $\tilde{L}_N(r, x; \theta)$ with respect to θ . The convergence of such optimization needs \tilde{L}_N to be continuous and differentiable in θ . This

is achieved by computing \tilde{L}_N for different values of θ under a set of common random numbers (CRNs), which means all the samplers $\{\tilde{\lambda}_t^{(i)}\}_{t=1}^T$ and $\{\lambda_t^{(i)}\}_{t=1}^T$ for different values of θ are obtained by transformation of a common set of canonical random numbers, here standardized normals. Once the parameters have been estimated, EIS can also be used to compute smoothed and filtered estimates of functions of λ_t .

The detailed algorithm of the implementation of EIS for this model is described as follows:

The EIS implementation for the likelihood evaluation of the TVP-RGARCH starts with the selection of the class of auxiliary samplers. Using a parametric extension of the initial sampler q given by Eq. (1.21), the corresponding density kernel of the Gaussian auxiliary sampler m can be parameterized as:

$$k(\lambda_t, \Lambda_{t-1}; \mathbf{a}_t) = q(\lambda_t | \Lambda_{t-1}; \theta) \zeta(\lambda_t; \mathbf{a}_t) \quad (1.27)$$

with

$$\zeta(\lambda_t; \mathbf{a}_t) = \mathbf{exp}(a_{1t} \lambda_t + a_{2t} \lambda_t^2) \quad (1.28)$$

where ζ is an auxiliary function, a_{1t} and a_{2t} are the importance sampling coefficients. Then the density kernel of the importance sampling auxiliary distribution has the form as:

$$k(\lambda_t, \Lambda_{t-1}; \mathbf{a}_t) = \begin{cases} \frac{1}{\sqrt{2\pi\gamma^2}} \mathbf{exp} \left\{ -\frac{1}{2} \left[\left(\frac{\delta\lambda_{t-1}}{\gamma} \right)^2 - 2 \left(\frac{\delta\lambda_{t-1}}{\gamma^2} + a_{1t} \right) \lambda_t \right. \right. \\ \left. \left. + \left(\frac{1}{\gamma^2} - 2a_{2t} \right) \lambda_t^2 \right] \right\}, & t : 2 \rightarrow T \\ \frac{1}{\sqrt{2\pi\gamma^2/(1-\delta^2)}} \left\{ -\frac{1}{2} \left[-2a_{11}\lambda_1 + \left(\frac{1-\delta^2}{\gamma^2} - 2a_{21} \right) \lambda_1^2 \right] \right\}, & t = 1 \end{cases} \quad (1.29)$$

Hence the auxiliary sampler is a Gaussian density, i.e., $m(\lambda_t | \lambda_{t-1}; \mathbf{a}_t) \sim N(\mu_t, \sigma_t^2)$, where

$$\mu_t = \sigma_t^2 \left(\frac{\delta\lambda_{t-1}}{\gamma^2} + a_{1t} \right), \quad \sigma_t^2 = \frac{\gamma^2}{1 - 2\gamma^2 a_{2t}} \quad t : 2 \rightarrow T, \quad (1.30)$$

and

$$\mu_1 = \sigma_1^2 a_{11}, \quad \sigma_1^2 = \frac{\nu^2}{1 - \delta^2 - 2\nu^2 a_{11}} \quad t = 1.$$

Integrating k_t with respect to λ_t leads, for the integrating constant, to

$$\chi(\Lambda_{t-1}; a_t) \propto \mathbf{exp} \left\{ \frac{\mu_t^2}{2\sigma_t^2} - \frac{\delta^2 \lambda_{t-1}^2}{2\nu^2} \right\}, \quad t : 2 \rightarrow T \quad (1.31)$$

Based on these functional forms, the computation of an EIS-MC estimate of the likelihood requires the following steps:

- Step 1: draw N independent trajectories $\{\check{\lambda}_1^{(i)}, \dots, \check{\lambda}_T^{(i)} : i = 1 \rightarrow N\}$ from the sequence of q distributions.
- Step 2: Use these trajectories to solve for each period $t : T \rightarrow 1$ the least squares problem defined in Eq. (1.26). The period t regression is:

$$\log p_t + \log \chi_{t+1} = c_t + a_{1t} \lambda_t^{(i)} + a_{2t} [\lambda_t^{(i)}]^2 + u_t^{(i)} \quad (1.32)$$

where $u_t^{(i)}$ denotes the regression error term and p_t is the density for $\{r_t, x_t\}$ given λ_t according to Eq. (1.20). The initial condition for the integrating constant is given by $\chi_{T+1}(\cdot) = 1$.

- Step 3: Use the estimates of the regression coefficients $\{\hat{a}_{1t}, \hat{a}_{2t}\}_{t=1}^T$ to obtain the Gaussian EIS sampler $m(\lambda_t | \Lambda_{t-1}; \hat{a}_t)$ characterized by the means and variances given by Eq. (1.29). Then generate N trajectories $\{\check{\lambda}_1^{(i)}, \dots, \check{\lambda}_T^{(i)} : i = 1 \rightarrow N\}$ from this EIS sampler from which the EIS-MC estimate of the likelihood is calculated according to Eq. (1.24)

Steps 1 to 3 should be iterated (about five times) to improve the efficiency of the approximations. This is done by replacing the natural sampler in Step 1 with the importance functions built in the previous iteration. (In our empirical analysis, the EIS parameters will converge after 2 or 3 iterations.)

Note that in Eq. (1.30), if $a_{2t} > 1/(2\mathcal{V}^2)$, ($a_{21} > (1 - \delta^2)/(2\mathcal{V}^2)$ when $t = 1$), the variance of the auxiliary sampler would be negative. To ensure the positiveness of the variances, we cannot simply do the OLS respect to the regression Eq. (1.32). In our application, a_{2t} is negative for most of the t 's. Thus here we impose the restriction $a_{2t} < 0$ on Eq. (1.32).

1.5 Simulation Study

In this section, we conduct a simulation study to illustrate the convergence of the ML-EIS estimators. We simulate data from the following specific TVP RGARCH model:

$$\begin{aligned}
 \text{Model 1} \quad & r_t = \sqrt{h_t} z_t, \quad z_t \sim N(0, 1) \\
 & \mathbf{\log} h_t = \omega_t + \beta_t \mathbf{\log} h_{t-1} + \gamma_t \mathbf{\log} x_{t-1} \\
 & \mathbf{\log} x_t = -0.01 + \mathbf{\log} h_t - 0.03 z_t + 0.12(z_t^2 - 1) + u_t \\
 & u_t \sim N(0, 0.04) \\
 & \begin{pmatrix} \omega_t \\ \beta_t \\ \gamma_t \end{pmatrix} = \begin{pmatrix} 0.14 \\ 0.5 \\ 0.3 \end{pmatrix} + \begin{pmatrix} 0.08 \\ 0.05 \\ 0.04 \end{pmatrix} \lambda_t \\
 & \lambda_t = 0.7\lambda_{t-1} + 0.2\eta_t \\
 & \eta_t \sim N(0, 1)
 \end{aligned}$$

In Model 1, r_t and x_t correspond to the daily return and realized measure of volatility, respectively. The value of the parameters $(d_1, d_2, d_3)'$ are chosen to be relatively small to prevent unsteady realization of $\log h_t$ and $\log x_t$.

1.5.1 Estimation

We simulate samples of length $T = 1,000$ and we split the samples into 800 observations as in-sample data and the remaining 200 observations as out-of-sample data. We do 100 replications,

with each replication having its own set of CRN ($N = 50$ trajectories combined with 5 iterations). According to Liesenfeld and Richard (2006), 50 trajectories are enough to for EIS to give an accurate approximation of the likelihood.

In Table 1.1, we report the mean and standard deviation of the estimates across the 100 replications. We also report standard errors based on asymptotic theory (number of CRN draws going to infinity and using the Hessian matrix of the log-likelihood). We also report the mean value of parameter estimates for the Realized GARCH model using these simulated series. The simulation results show that all the ML-EIS estimates are close to the true values of the parameters (with relatively small standard deviations), which suggests that we our implementation of EIS performs well for this model.

Next, we analyze the in-sample and out-of-sample estimates of time-varying parameters ω_t , β_t , and γ_t . Eq. (1.14) and (1.15) suggest that we could obtain the time-varying parameters from the common random variables η_t and the series of λ_t . We use the estimated parameters (see Table 1.1) and draw new CRNs to construct the in-sample and out-of-sample time-varying parameters. Since we have 50 trajectories of $\tilde{\lambda}_t^{(i)}$, we use the mean of the samples as the time series of λ_t . Then we can get ω_t , β_t , and γ_t from Eq. (1.14). The dynamics of in-sample and out-of-sample ω_t can be seen in Fig. 1.1 and 1.2, respectively. Since ω_t , β_t and γ_t are driven by a single series of λ_t , their dynamics are very similar to each other, and the plots look almost the same to each other. Thus, we just show the dynamics of ω_t . When we look at Fig. 1.1 and 1.2, which show the dynamics of both in-sample and out-of-sample ω_t , we see that the variation of the estimated $\hat{\omega}_t$ is not as large as the true ω_t . However, the estimated $\hat{\omega}_t$ captures the trend of the ω_t well. Thus we can see that the EIS method can successfully estimate the time-varying parameters in this context where we cannot get a closed form expression for the likelihood function.

Table 1.1: EIS Estimation of TVP Realized GARCH Model

Parameters	True Value	Mean of EIS Estimates	MC Std. Dev.	Mean of the S.E.	Mean of Realized GARCH Estimates
ω_0	0.14	0.1420	0.0148	0.0538	0.1905
β_0	0.5	0.4663	0.0120	0.0474	0.4746
γ_0	0.3	0.3487	0.0181	0.0632	0.2914
d_1	0.08	0.0393	0.1365	0.2087	
d_2	0.05	0.0103	0.2327	0.3320	
d_3	0.04	0.0510	0.2404	0.2055	
δ	0.7	0.6709	0.2908	0.2878	
ξ	-0.01	-0.0619	0.0481	0.1802	-0.2405
φ	1	1.0433	0.0601	0.2340	1.2492
τ_1	-0.03	-0.0375	0.0007	0.0063	-0.0368
τ_2	0.12	0.1228	0.0011	0.0095	0.1275
σ^2	0.04	0.0435	0.0008	0.0032	0.0444

The MC standard deviations are obtained from 100 replications of the ML-EIS estimation. The standard errors are based on asymptotic results ($N \rightarrow \infty$) and use the Hessian matrix of the log-likelihood. ML-EIS estimates are based on an MC sample size $N = 50$ and 5 iterations.

1.5.2 Forecast Performance Evaluation

We compare both in-sample and out-of-sample volatility predictions between our model and the benchmark Realized GARCH model. We use Mean Square Error (MSE) as the loss function to assess the forecasting performance:

$$MSE = \frac{1}{n} \sum_{i=1}^n (h_i - \hat{h}_i)^2 \quad (1.33)$$

The results shown in Table 1.2 imply that the in-sample and out-of-sample predictive ability is slightly better than the benchmark Realized GARCH model. This is an unsurprising result since the data is simulated from Model 1. Though both the in-sample and out-of-sample MSE depends on the newly drawn CRNs, our experience suggest that the in-sample and out-of-sample MSE barely varies with the random numbers.

Figure 1.1: In-Sample ω_t

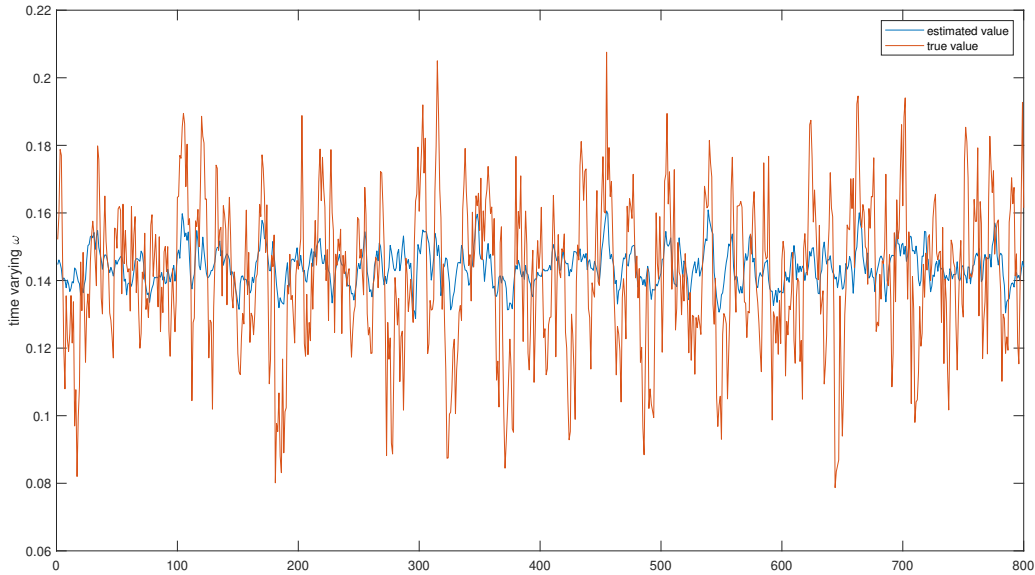


Table 1.2: Forecasting Performance

Models	in-sample MSE	out-of-sample MSE
realized GARCH	0.4329	0.7375
TVP realized GARCH	0.3988	0.7184

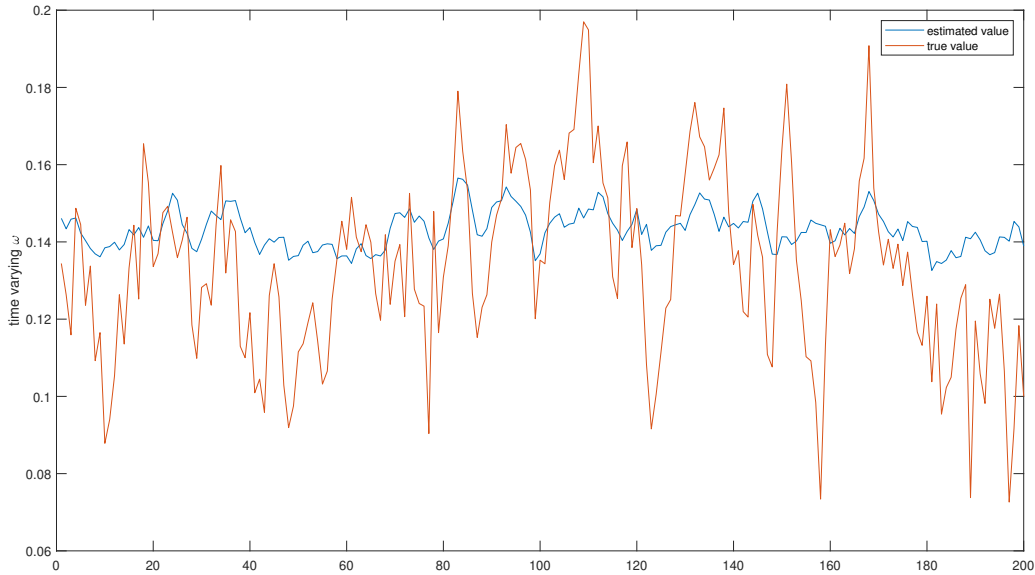
1.6 Empirical Analysis

We next apply estimate our model with daily returns and realized measures for different stock indices.

1.6.1 Data Description

We choose the realized library of the Oxford-Man Institute of Quantitative Finance as our data set. We selected the following 5 stocks indices with at least 4,000 daily observations: S&P 500 index (SPX), FTSE 100 (FTSE), EURO STOXX 50 (STOXX50E), Nikkei 225 (N225), OMX Stockholm All Share Index (OMXSPI), and Straits Times Index (STI). All of the series start in January 2000 and end in February 2022. The in-sample estimation period goes from November 23, 2017 to

Figure 1.2: Out-of-Sample ω_t



November 24, 2021. The out-of-sample period goes from November 25, 2021 to February 18, 2022.

We calculate the daily return as the first difference of daily close log-price, times 100. The descriptive statistics for the daily returns can be found in Table A.1. The averages of daily returns are very close to zero, and the difference between the minimum and maximum values of the daily returns are quite large. All the series are left skewed and leptokurtic. The plot of daily returns of the 6 stock indices in Figure A.1 illustrates the time-varying variances of these series.

The data set also contains daily realized measures of volatility computed with high-frequency returns for each stock index. Here we use the annualized realized variance computed with 5-minute returns (RV5), scaled by 100^2 so as to match our daily return series, for our estimation and forecasting. Descriptive statistics for RV5 are shown in Table A.2. The plots of RV5 of these series in Figure A.2 indicate a financial crisis in the first quarter of 2020.

1.6.2 Empirical Estimation Results

The estimated parameters for this model when applied to the six stock indices can be found in Table 1.3. First, let us look at the parameter δ for each of the stocks. With the small values of standard errors, all of the δ 's are statistically greater than zero for the stock indices. The parameter δ measures the persistence of the time-varying parameters ω_t , β_t and γ_t . The greater the value, the more persistent the time-varying parameters would be. According to the results, we could see that the OMX Stockholm All Share Index has the most persistent time-varying parameters ($\hat{\delta} = 0.6144$), while the S&P 500 Index has the least persistent parameters ($\hat{\delta} = 0.1464$).

Second, for the stock indices SPX, FTSE, STOXX50E and STI, the parameters in the GARCH equation, i.e., $(\omega, \beta, \gamma)'$, should be treated as time-varying, since at least one of the parameter loadings $(d_1, d_2, d_3)'$ are statistically non-zero at the significance level of 0.01. Whereas for the stock indices N225 and OMXSPI, none of the parameter loadings are statistically non-zero, thus the parameters $(\omega, \beta, \gamma)'$ could not be treated as time-varying. The absolute value of the loading parameters measures the range of variations for the time-varying parameters. For example, we have the greatest loading d_1 (the value is -0.3113) and the smallest loading d_2 (the value is 0.0675) for the S&P 500 Index, which indicates that the variation of ω_t is the greatest, while β_t does not vary as much.

Third, by allowing the loading parameters to be both positive and negative, the time-varying parameters in the GARCH equation could be changing in opposite directions, i.e. we might have ω_t going down while having β_t going up so that the mean of $\log h_t$ remains constant. What is interesting is that the parameters move in opposite directions for all stock indices, i.e., the signs of the parameters $(d_1, d_2, d_3)'$ are not all the same for all the stock markets.

Table 1.3: EIS Estimation of TVP Realized GARCH Model

Para		SPX	FTSE	STOXX50E	N225	OMXSPI	STI
ω_0	Estimate	0.4365	0.1072	0.1719	0.3876	0.3787	0.2918
	S.E.	0.1075	0.0126	0.0285	0.0854	0.1044	0.0032
β_0	Estimate	0.2869	0.6773	0.5534	0.5487	0.5664	0.5968
	S.E.	0.0506	0.0379	0.0376	0.0664	0.0632	0.0158
γ_0	Estimate	0.7257	0.2858	0.3892	0.3168	0.4468	0/4070
	S.E.	0.0474	0.0190	0.0095	0.0664	0.0664	0.0474
d_1	Estimate	-0.3113	-0.0068	-0.0631	-0.0067	0.0111	-0.0891
	S.E.	0.1391	0.0316	0.0538	0.0538	0.1360	0.0158
d_2	Estimate	0.0675	0.0731	0.1136	0.0560	0.0797	0.0063
	S.E.	0.0506	0.0095	0.0063	0.1138	0.0632	0.0065
d_3	Estimate	-0.1123	-0.0665	0.0583	0.0135	-0.0083	-0.0488
	S.E.	0.0443	0.0158	0.0980	0.0411	0.0696	0.0012
δ	Estimate	0.1464	0.5710	0.1923	0.3730	0.6144	0.5520
	S.E.	0.0126	0.0632	0.0095	0.0411	0.0158	0.0095
ξ	Estimate	-0.6647	-0.4182	-0.4968	-1.182	-0.8890	-0.8418
	S.E.	0.0411	0.0411	0.0379	0.0538	0.0379	0.0221
φ	Estimate	0.8450	0.9672	0.9427	1.156	0.8068	0.7698
	S.E.	0.0285	0.0474	0.0189	0.1012	0.0442	0.0160
τ_1	Estimate	-0.2760	-0.0726	-0.1452	-0.1421	-0.1541	-0.0850
	S.E.	0.0189	0.0190	0.0253	0.191	0.0153	0.0033
τ_2	Estimate	0.0824	0.1593	0.1305	0.1346	0.0640	0.0539
	S.E.	0.0131	0.0127	0.0124	0.0096	0.0094	0.0033
σ^2	Estimate	0.2279	0.3383	0.3387	0.2736	0.1861	0.1321
	S.E.	0.0155	0.0159	0.0194	0.0132	0.0102	0.0089

The standard errors are based on asymptotic theory ($N \rightarrow \infty$) and use the Hessian matrix of the log-likelihood. ML-EIS estimates are based on a MC sample size $N = 30$ and 5 iterations.

1.6.3 Forecasting Performance Comparison

Now we compare the out-of-sample forecasting performance between our model and the benchmark Realized GARCH model. Since we do not have the true conditional variances for the stock indices, according to Barndorff-Nielsen et al. (2009), we can use the realized kernel as the proxy of the conditional variance h_t . We still use MSE as the loss function in our empirical analysis. The results are shown in Table 1.5. We find that for the S&P 500 index, the FTSE 100

Table 1.4: Estimates of benchmark Realized GARCH Model

Parameters	SPX	FTSE	STOXX50E	N225	OMXSPI	STI
ω	0.4727	0.1271	0.2154	0.4052	0.4097	0.3786
β	0.3398	0.6727	0.5880	0.5431	0.5706	0.6088
γ	0.6821	0.2968	0.3654	0.3271	0.4631	0.4396
ξ	-0.7277	-0.4485	-0.5953	-1.120	-0.8992	-0.9010
φ	0.8538	0.9849	0.9825	1.192	0.8341	0.7964
τ_1	-0.2781	-0.0727	-0.1275	-0.1457	-0.1629	-0.0881
τ_2	0.0976	0.1582	0.1407	0.1300	0.0642	0.0466
σ^2	0.3010	0.3486	0.3916	0.2835	0.1932	0.1420

index and the Straits Times index, our model has a better forecasting performance than the benchmark Realized GARCH model (with a lower value of MSE), while for other stock indices, the benchmark model out-performs than our model in the volatility forecasting.

Table 1.5: Out-of-Sample MSE Comparison for All Stock Indices

	SPX	FTSE	STOXX50E	N225	OMXSPI	STI
Realized GARCH	3.4930	1.4261	1.6916	1.4916	2.1254	0.0291
TVP Realized GARCH	2.5529	1.3678	1.8146	1.6262	2.4472	0.0184

1.7 Conclusion

In this paper, we extend the Realized GARCH model to the Time-varying parameter realized GARCH model by letting the parameters in the GARCH equation be time-varying and driven by a single sequence of latent variables. We apply the efficient importance sampling method to estimate the parameters of our model and through simulations we illustrate that this method provides accurate estimates. When applying our model to real financial data, we find that all parameters in the GARCH equation should be treated as time-varying. Moreover, forecasting performance comparisons suggest that in some cases our model would outperforms the benchmark Realized GARCH model.

We could further extend the model to a more general case. For example, it could be interesting to let the parameters in the GARCH equation follow three independent AR(1) processes or we could let all the parameters in the GARCH and measurement equations be time-varying.

CHAPTER

2

DOES VIX HAVE ADDITIONAL INFORMATION TO REALIZED VOLATILITY? EVIDENCE FROM S&P 500 AND VIX INDEX

2.1 Introduction

Volatility forecasting is still playing an important role in today's empirical finance research. Access to accurate volatility forecasts is of the utmost importance for many financial market practitioners and regulators, and a number of models have been introduced and revised for the purpose of forecasting future volatility. One approach to measure and forecast the volatility is the family of stochastic volatility models (see Taylor (2007)). For example, Stein and Stein (1991)

derive an explicit closed-form solution for the stochastic volatility following AR(1) process and applied their results to options pricing volatility; Andersen (1994) introduced an extended model called the stochastic autoregressive volatility (SARV) model and applied this model along with the Kalman Filter procedure in the volatility forecast based on the bivariate return-volume series; a new way of modeling stochastic volatility with Markov-switching was proposed by So et al. (1998), estimated with Bayesian method, and this approach successfully explains the persistence in volatility within different regimes; Barndorff-Nielsen and Shephard (2002) introduced realized volatility in the SV model and increased the accuracy in the estimation of "actual volatility"; and more recently, Luo et al. (2018) applied neural network to SV model and the empirical results showed that this new method outperforms conventional models in estimation and prediction in stock volatility.

The other popular approach to measure and predict volatility is the family of GARCH models. The GARCH model (see Bollerslev (1986)) can be also regarded as a category of the SV model, with a certain correlation between volatility series in discrete time periods. Many scholars have developed the GARCH type models to get a more accurate prediction in volatility, for example, Nelson (1991) introduced the exponential GARCH (EGARCH) model and applied this model to the estimation of the risk premium on the CRSP Value-Weighted Market Index from 1962 to 1987; Engle and Ng (1993) developed an asymmetric GARCH (AGARCH) model which emphasizes the asymmetry of stock volatility response to news; Glosten et al. (1993) modified the GARCH model by allowing different impacts on conditional volatility between positive and negative returns, which is later called the GJR-GARCH model; Zakoian (1994) extended the GARCH model to the Threshold GARCH (TGARCH) model in which the conditional standard deviation is a piecewise linear function of past values of the white noise, and applied it to the French CAC index by comparing the results with other categories of GARCH models.

Our method in this chapter is based on the Realized GARCH model. The Realized GARCH model is introduced by Hansen et al. (2011), incorporating realized volatility into the GARCH model. With an additional source of information included in the model, the Realized GARCH

model is more efficient in short-term volatility forecasting, especially within 7 days. Wang et al. (2022) extended this model to the Realized GARCH-RSRK model by including realized higher moments - the realized skewness and the realized kurtosis - into the model. The VaR forecast results show that the realized higher moments do contain additional information over the realized volatility so it outperformed the benchmark model in forecasting the VaR.

In this article, we explore the effect of including implied volatility (VIX index) into the realized GARCH model, with the purpose of seeing whether the inclusion of the implied volatility improves forecast performance. In other words, we are looking into the question whether the implied volatility has incremental information over and above the benchmark Realized GARCH model that is useful in the future volatility forecast.

Many researchers have tried to establish a link between the GARCH family models and the VIX index. Some of them tried to use the GARCH family models to obtain the model implied VIX index, for example, Hao and Zhang (2013) derived the formula for the GARCH model implied VIX index, and found that the model implied VIX index is consistently and significantly lower than the COBE VIX index. Hansen et al. (2022) got the model implied VIX index under the Realized GARCH model and it proved that the realized volatility plays an important role in forecasting the VIX index. On the other hand, a few researchers attempted to incorporate the VIX index into the GARCH family models to improve the forecast performance. By extracting the daily spot volatility of GARCH model from the series of VIX instead of linking spot volatility with different dates, Kannianen et al. (2014) found that the new model outperforms the benchmark GARCH model in pricing options on the S&P 500 index. Kambouroudis and McMillan (2016) incorporate the VIX index and the trading volume into many GARCH family models, and the results show that either VIX or volume could provide additional forecast power.

Though it has been shown that either realized volatility or VIX can improve the forecasting performance of GARCH family models, few have combined these two kinds of volatility together into a single model. In this chapter, we aim to examine whether including both types of volatility jointly could improve volatility forecasting performance compared to including only one of

them in a GARCH model.

The rest of this article is organized as follows: in section 2, we review in more details the VIX index; in section 3, we construct the Realized GARCH-VIX model; section 4 gives the likelihood and the estimation method of our new model; in section 5, we compare both the in-sample and out-of-sample volatility forecasting performance between our model and the benchmark Realized GARCH model; section 6 concludes and proposes potential future extensions.

2.2 VIX Index: a Review

The COBE volatility index (VIX) was introduced in 1993 and measures the expected volatility of S&P 100 Index over the next 30 calendar days, computed on a real-time basis from the implied volatility of option prices. Unlike normal stock indices, VIX is not a tradable financial asset. Instead, it is commonly described as a “fear index” (see Engle (2004) and Simons (2003)). In 2003, COBE updated the calculation of VIX using S&P 500 (SPX) options by averaging the weighted prices of SPX puts and calls over a wide range of out-of-the-money strike prices. This change has made VIX a standard for trading and hedging volatility.

To understand VIX, it is important to learn that it is a forward-looking measure of volatility that traders expect to see. The value of VIX (“fear index”) indicates the market’s expectation of 30-day forward volatility. Higher VIX levels imply a greater “fear” in the market. According to Hancock (2012), the “fear index” is generally believed to conform to the following interpretations: The more detailed algorithm used to calculate the VIX is described in Appendix B.

Sometimes the VIX index is naively interpreted as the prediction for the annualized realized measure of volatility over the next 30 days. However, when we look at Fig. 2.1, which depicts the VIX index and annualized realized volatility from Nov. 30, 2007 to Nov. 23, 2009, it seems that the trend of the VIX index does not forecast the direction of realized volatility. For example, during the financial crisis in year 2008, the realized volatility peaks on Oct. 10, 2008, while

FEAR INDEX	
5-10	extreme complacency
10-15	very low anxiety/high complacency
15-20	low anxiety/moderate complacency
20-25	moderate anxiety/low complacency
25-30	moderately high anxiety
30-35	high anxiety
35-40	very high anxiety
40-45	extremely high anxiety
45-50	near panic
50-55	moderate panic
55-60	panic
60-65	intense panic
65+	extreme panic

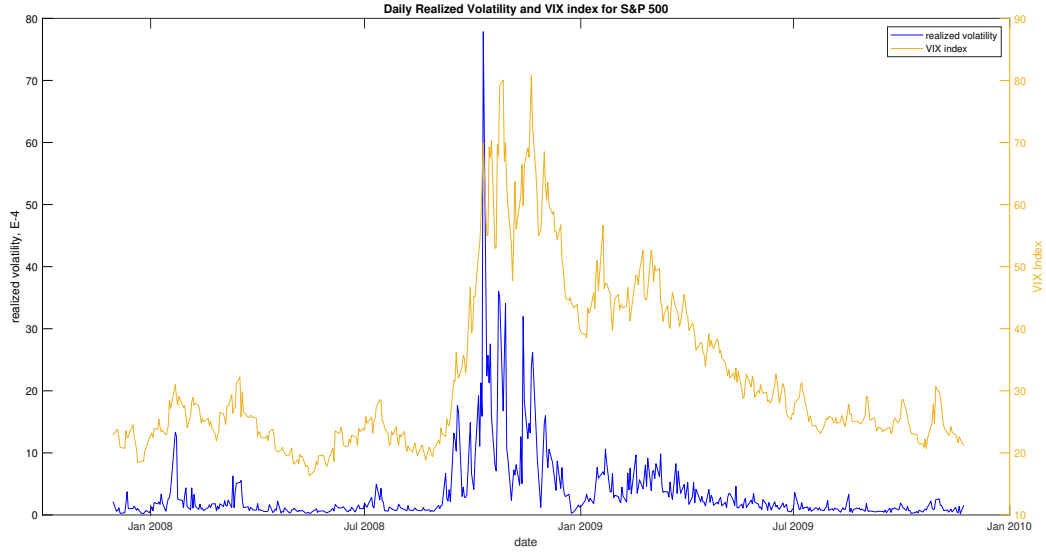
the VIX index peaks at the same day. Thus the VIX index does not predict the financial crisis, instead, it responds to the financial crisis, just like the realized volatility. The logic behind this is that both implied and realized volatility are based on the information before time t , so it could not be treated as a prediction for time $t + 1$.

The VIX index indicates the implied volatility over the next 30 calendar days, whereas the realized volatility (RV) measures the variance within a single day. In order to incorporate them into our empirical model, we need to normalize the VIX index to the same time scale as realized volatility. The normalized VIX is defined as:

$$VIX_{norm} = (VIX * \frac{1}{C})^2 \quad (2.1)$$

where C is the annualized factor given by $C = 100\sqrt{252}$. And thus the daily realized volatility. The normalized IV denotes the daily implied volatility derived from the annualized VIX index. Fig. 2.2 shows the comparison between daily implied volatility and realized volatility.

Figure 2.1: VIX vs. Realized Volatility



2.3 Model Specification

Our model is based on the exponential Realized GARCH model introduced by Hansen et al. (2011):

$$r_t = \sqrt{h_t} z_t \quad (2.2)$$

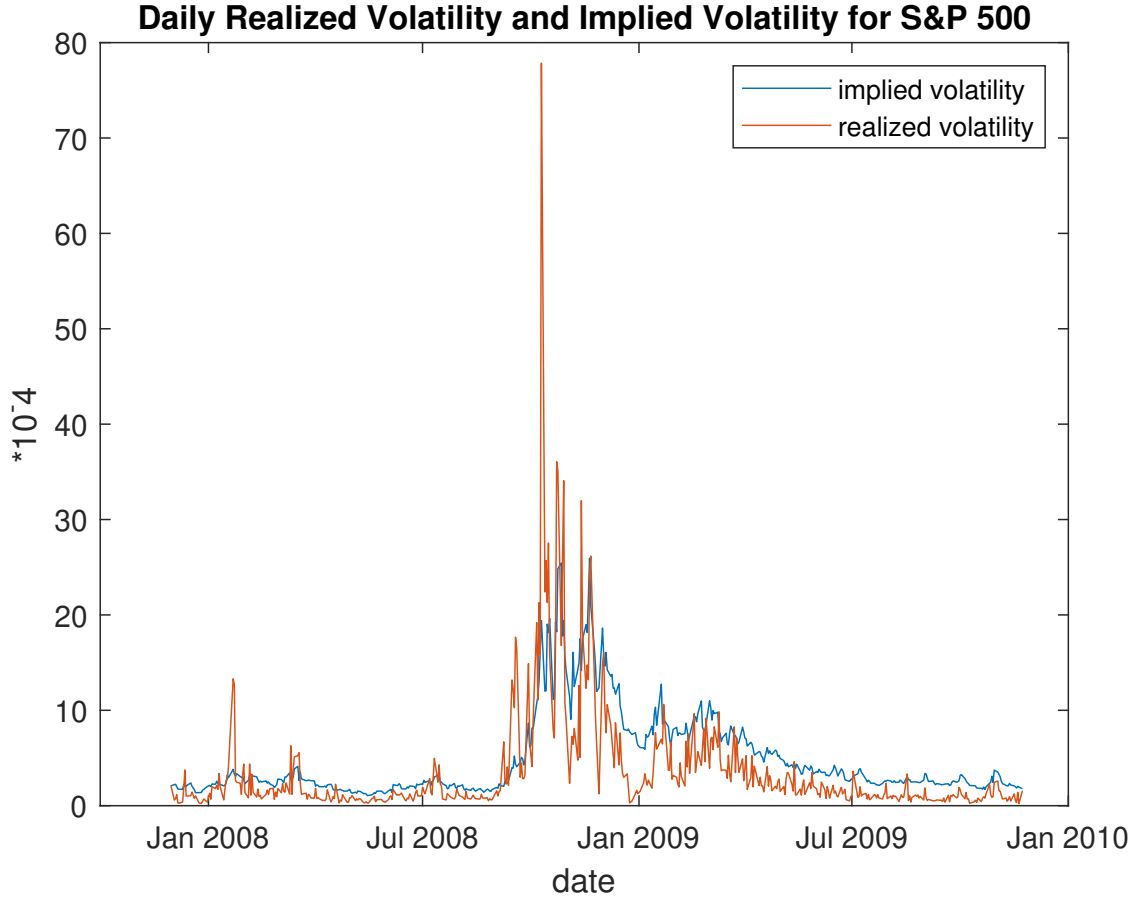
$$\mathbf{\log} h_t = \omega + \beta \mathbf{\log} h_{t-1} + \gamma \mathbf{\log} x_{t-1} \quad (2.3)$$

$$\mathbf{\log} x_t = \xi + \varphi \mathbf{\log} h_t + \tau(z_t) + u_t \quad (2.4)$$

where r_t denotes the daily returns with $\mathbb{E}[r_t | \mathcal{F}_{t-1}] = 0$, $h_t = \mathbb{E}[r_t^2 | \mathcal{F}_{t-1}]$ (\mathcal{F}_{t-1} is the information set up to time $t-1$) is the conditional variance of daily returns, x_t denotes the realized measure of volatility. The random errors z_t and u_t are assumed to be independent, with $z_t \sim N(0, 1)$ and $u_t \sim N(0, \sigma_u^2)$. Finally, $\tau(z_t) = \tau_1 z_t + \tau_2 (z_t - 1)^2$ denotes the leverage effect, which captures the dependence between returns and future volatility.

Inspired by the GARV model proposed by Christoffersen et al. (2014), we introduce our new

Figure 2.2: Normalized VIX vs. Realized Volatility



model called Realized GARCH-VIX model. The model is defined as follows:

$$r_t = \sqrt{h_t} z_t \quad (2.5)$$

$$h_t = \kappa h_t^V + (1 - \kappa) h_t^{RV} \quad (2.6)$$

$$\log h_t^V = \omega_1 + \beta_1 \log h_{t-1}^V + \gamma_1 \log v_{t-1} \quad (2.7)$$

$$\log h_t^{RV} = \omega_2 + \beta_2 \log h_{t-1}^{RV} + \gamma_2 \log x_{t-1} \quad (2.8)$$

$$\log v_t = \xi_1 + \varphi_1 \log h_t^V + \tau(z_t) + \epsilon_t \quad (2.9)$$

$$\log x_t = \xi_2 + \varphi_2 \log h_t^{RV} + \tau(z_t) + u_t \quad (2.10)$$

where v_t denotes the normalized VIX index as reviewed in Section 2, $\epsilon_t \sim N(0, \sigma_\epsilon^2)$ is normally distributed and independent of u_t , and $u_t \sim N(0, \sigma_u^2)$.

The key idea of this model is that the conditional variance of the daily return, h_t , consists of two components. The first component, h_t^V , is driven by the VIX index, and the second component, h_t^{RV} , is driven by realized volatility. Eq. (2.9) and (2.10) are two measure equations that link realized volatility and implied volatility to the corresponding conditional variance, respectively.

According to Hao and Zhang (2013), the VIX can be calculated as the annualized arithmetic average of the expected daily variance over the following month under \mathbb{Q} measure:

$$VIX_t = A \times \sqrt{\sum_{k=1}^{22} \mathbb{E}_t^{\mathbb{Q}}[h_{t+k}]}$$

where A is the annualized factor given by $A = 100\sqrt{\frac{252}{22}}$.

On the other hand, Huang et al. (2020) also derived the VIX formula implied in the Realized GARCH model:

$$VIX_t = A \times \sqrt{\sum_{k=1}^{22} F_k h_{t+k}^{\beta^{k-1}}} \quad (2.11)$$

where

$$F_k = \exp\left[\frac{\omega(1 - \beta^{k-1})}{1 - \beta} + \sum_{i=0}^{k-2} \log[\Delta(\beta^i)]\right]$$

2.4 Model Estimation

We estimate our model with quasi maximum likelihood estimation (QMLE) method.

2.4.1 Likelihood of Realized GARCH Model

Following Hansen et al. (2011), the log-likelihood function of the Realized GARCH model is given by:

$$\ell(r, x|\theta) = -\frac{1}{2} \sum_{t=1}^T \left(\log h_t + \frac{r_t^2}{h_t} + \log \sigma_u^2 + \frac{u_t^2}{\sigma_u^2} \right) \quad (2.12)$$

We could separate the log-likelihood $\ell(r, x|\theta)$ into two components, $\ell(r|\theta)$ and $\ell(x|\theta)$, respectively, where

$$\ell(r|\theta) = -\frac{1}{2} \sum_{t=1}^T \left(\log h_t + \frac{r_t^2}{h_t} \right) \quad (2.13)$$

$$\ell(x|\theta) = -\frac{1}{2} \sum_{t=1}^T \left(\log \sigma_u^2 + \frac{u_t^2}{\sigma_u^2} \right) \quad (2.14)$$

so that

$$\ell(r, x|\theta) = \ell(r|\theta) + \ell(x|\theta),$$

where θ denotes the parameters to be estimated.

2.4.2 Likelihood of Realized GARCH-VIX Model

The log-likelihood function of Realized GARCH-VIX consists of three parts:

$$\ell(r|\theta) = -\frac{1}{2} \sum_{t=1}^T \left(\log h_t + \frac{r_t^2}{h_t} \right) \quad (2.15)$$

$$\ell(x|\theta) = -\frac{1}{2} \sum_{t=1}^T \left(\log \sigma_u^2 + \frac{u_t^2}{\sigma_u^2} \right) \quad (2.16)$$

$$\ell(v|\theta) = -\frac{1}{2} \sum_{t=1}^T \left(\log \sigma_\epsilon^2 + \frac{\epsilon_t^2}{\sigma_\epsilon^2} \right) \quad (2.17)$$

Then the likelihood function of our model can be written as:

$$\ell(r, x, v|\theta) = \ell(r|\theta) + \ell(x|\theta) + \ell(v|\theta) \quad (2.18)$$

Since h_t , h_t^V and h_t^{RV} are latent variables that could not be observed, here we assume all the latent volatility at the initial time period is equal to the unconditional variance of the daily returns, i.e., $h_1 = h_1^V = h_1^{RV} = VAR(r_t)$. As a result, here we do not maximize the log-likelihood through period 1 to T , but the log-likelihood from period 2 to T conditioning on the first time period. The conditional log-likelihood is given by:

$$\ell(r, x, v|\theta; \mathcal{F}_1) = -\frac{1}{2} \sum_{t=2}^T \left(\log h_t + \frac{r_t^2}{h_t} + \log \sigma_u^2 + \frac{u_t^2}{\sigma_u^2} + \log \sigma_\epsilon^2 + \frac{\epsilon_t^2}{\sigma_\epsilon^2} \right) \quad (2.19)$$

where \mathcal{F}_1 is the information set of time period 1, and all the latent volatility $\{h_t\}_{t=2}^T$ could be constructed by the parameters and the initial values of h_1 , h_1^V and h_1^{RV} .

2.5 Data and Empirical Results

2.5.1 Data Description

We select the S&P 500 index from Dec 2007 to Nov 2013, giving us 1500 observations. The daily realized volatility are chosen from the Oxford Realized Library and we use the 10-min sub-sampled RV in our model. Descriptive statistics can be found in Table 2.1.

The time series of the VIX index and daily realized volatility is shown in Fig. 2.1, and the time series of daily normalized VIX vs. daily realized volatility can be seen in Fig. 2.2. Fig. 2.2 indicates that the daily implied volatility does not vary as much as daily realized volatility, and both of them move in the same directions from a long-term scope, though they may move in opposite directions in some short-term time periods. During the financial crisis in 2008, both implied volatility and realized volatility reach their highest values.

2.5.2 Parameter Estimates

We select the first 1000 observations as in-sample data, and the remaining 500 observations as out-of-sample data. Table 2.2 shows the in-sample estimation results for both standard

Table 2.1: Descriptive Statistics

	T	Min	Median	Mean	Max	SD	Kurtosis	Skewness
daily return (r_t)	1500	-9.688	0.0798	0.0126	10.64	1.528	10.67	-0.2391
realized volatility (x_t)	1500	0.0400	0.7217	1.7926	77.84	3.928	115.1	8.209
VIX index	1500	11.30	20.98	24.02	80.86	10.91	7.638	1.979
normalized VIX (v_t)	1500	0.5067	1.746	2.762	25.95	3.115	17.24	3.387

Realized GARCH model and the Realized GARCH-VIX model.

Table 2.2: Estimation Results

Parameters	realize GARCH	Realized GARCH-VIX
κ		0.3573
ω_1		-0.0265
β_1		0.0593
γ_1		0.8734
ω_2	0.1815	-0.0152
β_2	0.6112	0.4700
γ_2	0.3786	0.5333
ξ_1		0.0485
φ_1		1.054
ξ_2	-0.4373	0.0337
φ_2	0.9545	0.9051
τ_1	0.3033	-0.1157
τ_2	-0.0852	0.0168
σ_v^2		0.0060
σ_u^2	0.1669	0.3285

2.5.3 Forecasting Performance

Figs. 2.3 and 2.4 show the in-sample and out-of-sample forecasting performance of our model, respectively. We found that for both in-sample and out-of-sample prediction, the predicted volatility is very close to the actual volatility (denoted by the realized kernel), and our model can capture the trend of the actual volatility very well.

We compare both in-sample and out-of-sample forecasting performance for the two models. We apply the following loss functions to test the predictive ability of our models:

$$MSE = \frac{1}{n} \sum_{i=1}^n (h_i - \hat{h}_i)^2 \quad (2.20)$$

The in-sample and out-of-sample prediction results are shown in table 2.3.

Table 2.3: In-Sample Forecasting Performance

	in-sample MSE	out-of-sample MSE
Realized GARCH	15.06	0.3199
Realized GARCH-VIX	9.76	0.1921

Figure 2.3: In-Sample Forecasting Performance of Realized GARCH-VIX Model

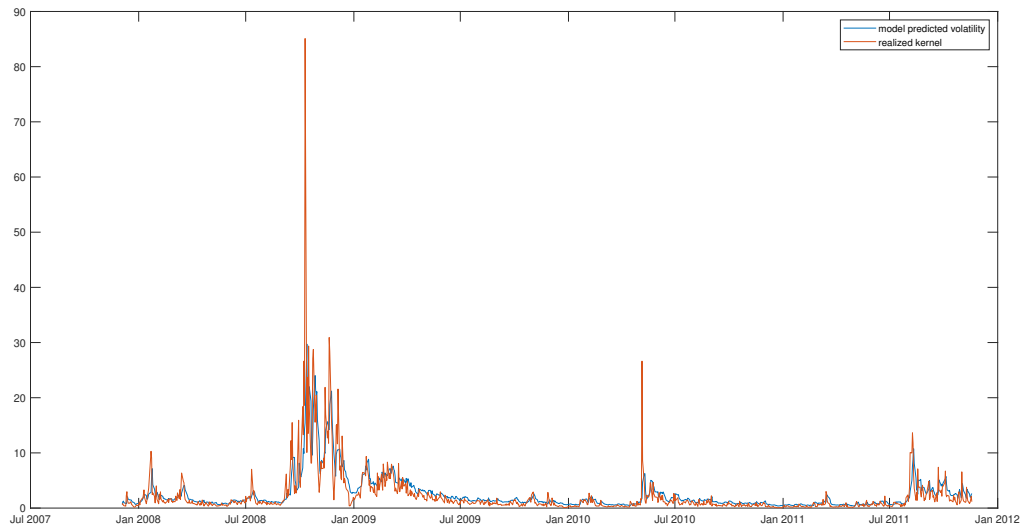
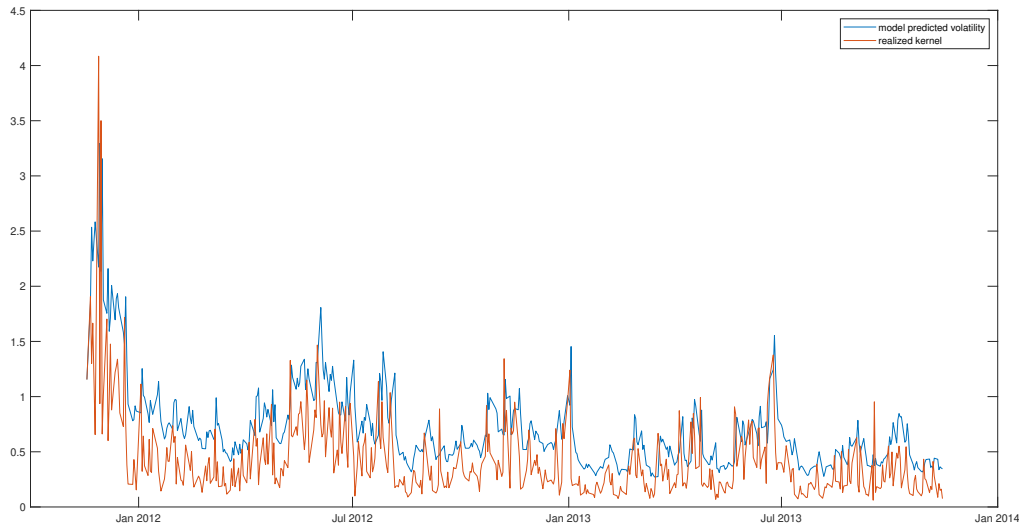


Figure 2.4: Out-of-Sample Forecasting Performance of Realized GARCH-VIX Model



2.5.4 Estimation and Forecasting in Rolling Windows

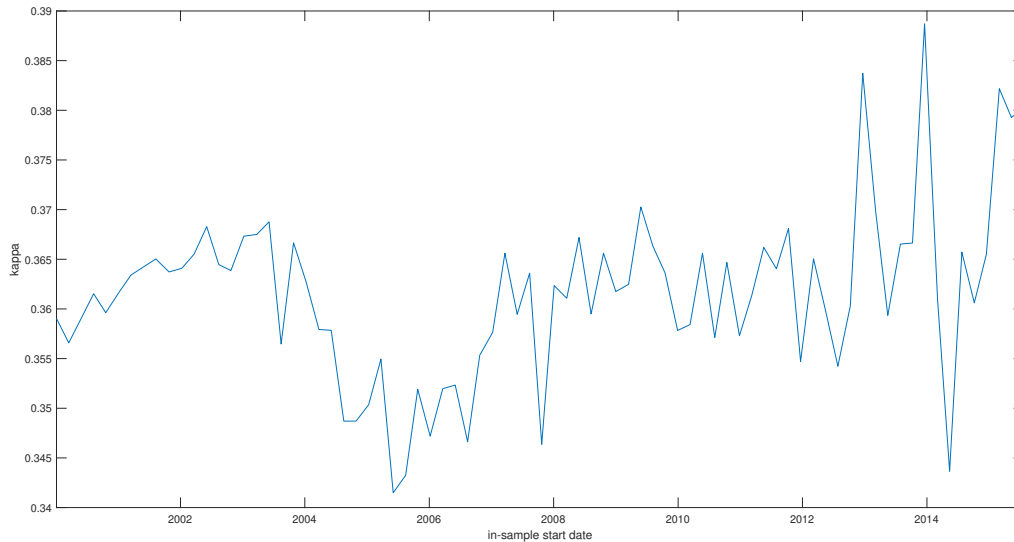
Now we consider the whole sample of data, from January 2000 to November 2021. To test the robustness of our results, we estimate our model with a rolling window (1000 in-sample observations and 500 out-of-sample observations, moving forward in 50 observations increments), and compare the out-of-sample MSE between the two models. In total, we have 79 windows.

Time-Varying κ

Fig. 2.5 shows the variation of the estimates of parameter κ over the windows. This parameter κ does not change a lot over time and it fluctuates between 0.34 and 0.39, and the average value is about 0.36, which means that the VIX contributes about 36% of the conditional variance, while the realized volatility contributes about 64%. Compared with the benchmark Realized GARCH model, the VIX offers more information in the explanation and forecasting of total volatility. In addition, the small range of κ suggests that our model is stable over time, and the parameter would not change much in the future. Thus, we could use this model to do a robust

future volatility prediction.

Figure 2.5: Time Varying κ



This figure shows the parameter κ changes over the rolling windows.

MSE Difference

The MSE differences are shown in Table 2.4.

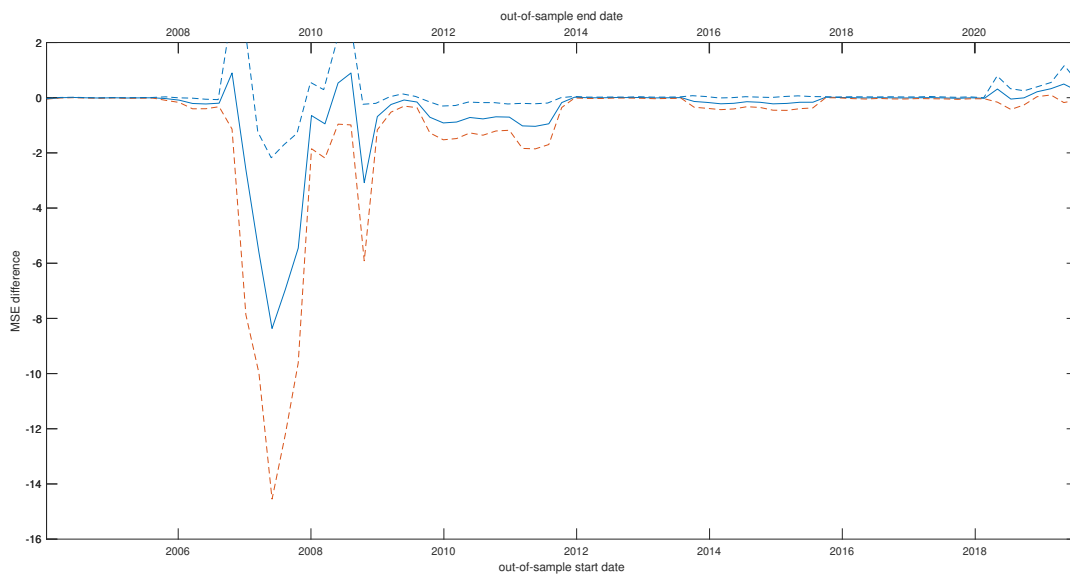
According to FRED Economic Data, there are two recessions during our sample: 2008Q1 to 2009Q3 and 2020Q1 to 2020Q2. The out-of-sample periods of Windows 12-29 out-of-sample periods contain the financial crisis of 2008Q1-2009Q3 and Windows 72-79 out-of-sample periods of 2020Q1-2020Q2 contain the COVID-19 recession. The out-of-sample MSEs are fairly larger during the recessions than in other periods, especially during the 2008 financial crisis, with this crisis lasting for longer than the COVID-19 recession.

What we care most about is the MSE difference between the two models. The column "MSE difference" is defined as the MSE of Realized GARCH-VIX model minus the MSE of the benchmark Realized GARCH model. Thus, if the MSE difference is less than zero, that means

our model outperforms the benchmark Realized GARCH model in future volatility prediction. Table 2.4 shows that the MSE differences of 60 rolling windows out of 79 are less than 0, which means that for most of the windows, our model generates more precise volatility forecasts than the benchmark model.

The column "t-value" reports the t-statistic of the MSE difference, which is obtained from the Diebold-Mariano test (see Appendix C). The results indicate that for 24 out of 60 rolling windows, the forecasting accuracy is statistically better than the benchmark model at a 10% significance level. Fig. 2.6 shows the MSE difference of the two models and the 90% confidence interval. We could see that the MSE differences are close to zero except when the financial crisis is included in the out-of-sample period. This result suggests that our model could provide a more accurate prediction during a financial crisis.

Figure 2.6: MSE Difference for Rolling Windows



This figure shows the MSE of our model minus the MSE of the benchmark Realized GARCH model (the middle blue line) over the rolling windows, and the 10% confidence interval of the MSE differences (the dashed lines).

Table 2.4: Out-of-Sample Forecasting Performance in Rolling Windows

rolling window index	in-sample start date	in-sample end date	out-of-sample start date	out-of-sample end date	MSE for GARCH	MSE for GARCH-VIX	MSE difference	t-value
1	2000-01-04	2004-01-07	2004-01-08	2006-01-05	0.0932	0.0526	-0.0406	-6.722
2	2000-03-16	2004-03-23	2004-03-24	2006-03-20	0.0756	0.0756	-0.0000	-0.0009
3	2000-05-30	2004-06-03	2004-06-24	2006-06-01	0.0573	0.0655	0.0082	1.734
4	2000-08-09	2004-08-16	2004-08-27	2006-08-11	0.0636	0.0591	-0.0045	-0.9489
5	2000-10-19	2004-10-27	2004-10-28	2006-10-23	0.0662	0.0550	-0.0112	-2.622
6	2001-01-02	2005-01-07	2005-01-10	2007-01-05	0.0569	0.0548	-0.0021	-0.5503
7	2001-03-16	2005-03-22	2005-03-27	2007-03-20	0.0817	0.0707	-0.0110	-1.636
8	2001-05-30	2005-06-02	2005-06-03	2007-05-31	0.0773	0.0711	-0.0062	-0.9817
9	2001-08-09	2005-08-12	2005-08-15	2007-08-10	0.0993	0.0967	-0.0026	-0.0424
10	2001-10-26	2005-10-24	2005-10-25	2007-10-22	0.2021	0.1695	-0.0326	-0.8412
11	2002-01-09	2006-01-05	2006-01-06	2008-01-03	0.3109	0.2226	-0.0882	-1.742
12	2002-03-22	2006-03-20	2006-03-21	2008-03-17	0.7195	0.5101	-0.2094	-1.783
13	2002-06-24	2006-06-01	2006-06-02	2008-05-28	0.7810	0.5537	-0.2273	-2.166
14	2002-08-14	2006-08-11	2006-08-14	2008-08-07	0.8009	0.6021	-0.1987	-2.554
15	2002-10-24	2006-10-23	2006-10-24	2008-10-17	13.03	13.93	0.8963	0.7249

Table 2.4 (Continued): Out-of-Sample Forecasting Performance in Rolling Windows

16	2003-01-08	2007-01-05	2007-01-08	2008-12-30	20.62	18.02	-2.597	-0.8114
17	2003-03-25	2007-03-20	2007-03-21	2009-03-13	24.67	19.06	-5.612	-2.111
18	2003-06-05	2007-05-31	2007-06-01	2009-05-26	28.36	20.00	-8.365	-2.224
19	2003-08-15	2007-08-10	2007-08-13	2009-08-05	26.74	19.79	-6.951	-2.177
20	2003-10-27	2007-10-22	2007-10-23	2009-10-15	25.52	20.07	-5.451	-2.155
21	2004-01-08	2008-01-03	2008-01-04	2009-12-28	20.40	19.75	-0.6474	-0.8858
22	2004-03-24	2008-03-17	2008-03-18	2010-03-11	19.30	18.35	-0.9479	-1.259
23	2004-06-24	2008-05-28	2008-05-29	2010-05-21	19.49	20.02	0.5316	0.5867
24	2004-08-27	2008-08-07	2008-08-08	2010-08-03	18.90	19.80	0.8953	0.7827
25	2004-10-28	2008-10-17	2008-10-20	2010-10-13	8.777	5.697	-3.080	-1.783
26	2005-01-10	2008-12-30	2008-12-31	2010-12-23	2.940	2.255	-0.6851	-2.343
27	2005-03-27	2009-03-13	2009-03-16	2011-03-08	2.328	2.081	-0.2471	-1.468
28	2005-06-03	2009-05-26	2009-05-27	2011-05-18	1.966	1.883	-0.0830	-0.6152
29	2005-08-15	2009-08-05	2009-08-06	2011-07-29	1.924	1.767	-0.1570	-1.269
30	2005-10-25	2009-10-15	2009-10-16	2011-10-10	3.073	2.365	-0.7079	-2.047
31	2006-01-06	2009-12-28	2009-12-29	2011-12-20	3.417	2.503	-0.9143	-2.459
32	2006-03-21	2010-03-11	2010-03-12	2012-03-05	3.415	2.533	-0.8818	-2.422
33	2006-06-02	2010-05-21	2010-05-24	2012-05-15	1.958	1.241	-0.7172	-2.111

Table 2.4 (Continued): Out-of-Sample Forecasting Performance in Rolling Windows

34	2006-08-14	2010-08-03	2010-08-04	2012-07-26	1.884	1.116	-0.7681	-2.138
35	2006-10-24	2010-10-13	2010-10-14	2012-10-05	1.793	1.100	-0.6925	-2.217
36	2007-01-08	2010-12-23	2010-12-27	2012-12-29	1.771	1.067	-0.7037	-2.429
37	2007-03-21	2011-03-08	2011-03-09	2013-03-05	2.127	1.106	-1.021	-2.058
38	2007-06-01	2011-05-18	2011-05-19	2013-05-15	2.082	1.045	-1.038	-2.088
39	2007-08-13	2011-07-29	2011-08-01	2013-07-26	1.948	1.002	-0.9455	-2.068
40	2007-10-23	2011-10-10	2011-10-11	2013-10-07	0.5867	0.4094	-0.1773	-1.639
41	2008-01-04	2011-12-20	2011-12-21	2013-12-17	0.1932	0.2113	0.0181	1.054
42	2008-03-18	2012-03-05	2012-03-06	2014-03-03	0.1669	0.1646	-0.0023	-0.1608
43	2008-05-29	2012-05-15	2012-05-16	2014-05-13	0.1549	0.1511	-0.0037	-0.2518
44	2008-08-08	2012-07-26	2012-07-27	2014-07-24	0.1150	0.1214	0.0064	0.5433
45	2008-10-20	2012-10-05	2012-10-08	2014-10-03	0.0977	0.1022	0.0045	0.4465
46	2008-12-31	2012-12-19	2012-12-20	2014-12-15	0.1159	0.1233	0.0073	0.4363
47	2009-03-16	2013-03-05	2013-03-26	2015-02-27	0.1341	0.1261	-0.0080	-0.4643
48	2009-05-27	2013-05-15	2013-05-16	2015-05-11	0.1257	0.1231	-0.0027	-0.1808
49	2009-08-06	2013-07-26	2013-07-29	2015-07-22	0.1237	0.1268	0.0031	0.2108
50	2009-10-16	2013-10-07	2013-10-08	2015-10-01	0.5237	0.3874	-0.1363	-1.073
51	2009-12-29	2013-12-17	2013-12-18	2015-12-11	0.5526	0.3818	-0.1708	-1.308

Table 2.4 (Continued): Out-of-Sample Forecasting Performance in Rolling Windows

52	2010-03-12	2014-03-03	2014-03-04	2016-02-25	0.6627	0.4417	-0.2210	-1.714
53	2010-05-24	2014-05-13	2014-05-14	2016-05-06	0.6366	0.4336	-0.2031	-1.632
54	2010-08-04	2014-07-24	2014-07-25	2016-07-19	0.6324	0.4874	-0.1450	-1.316
55	2010-10-14	2014-10-03	2014-10-06	2016-09-28	0.6275	0.4610	-0.1665	-1.461
56	2010-12-27	2014-12-15	2014-12-16	2016-12-08	0.6506	0.4280	-0.2226	-1.585
57	2011-03-09	2015-02-27	2015-03-02	2017-02-22	0.6304	0.4233	-0.2071	-1.352
58	2011-05-19	2015-05-11	2015-05-12	2017-05-04	0.6214	0.4561	-0.1653	-1.171
59	2011-08-01	2015-07-22	2015-07-23	2017-07-17	0.5793	0.4150	-0.1643	-1.311
60	2011-10-11	2015-10-01	2015-10-02	2017-09-26	0.1249	0.1426	0.0117	1.633
61	2011-12-21	2015-12-11	2015-12-14	2017-12-06	0.1020	0.1115	0.0095	0.9981
62	2012-03-06	2016-02-25	2016-02-16	2018-02-20	0.1596	0.1599	0.0003	0.0157
63	2012-05-16	2016-05-06	2016-05-09	2018-05-02	0.1723	0.1640	-0.0083	-0.3479
64	2012-07-27	2016-07-19	2016-07-20	2018-07-13	0.1598	0.1601	0.0004	0.0215
65	2012-10-08	2016-09-28	2016-09-29	2018-09-25	0.1611	0.1559	-0.0053	-0.2243
66	2012-12-20	2016-12-08	2016-12-09	2018-12-05	0.1889	0.1790	-0.0099	-0.4409
67	2013-03-26	2017-02-22	2017-02-23	2019-02-20	0.2131	0.2111	-0.0020	-0.1131
68	2013-05-16	2017-05-04	2017-05-05	2019-05-02	0.2137	0.2161	0.0024	0.0973
69	2013-07-29	2017-07-17	2017-07-18	2019-07-16	0.2192	0.2105	-0.0087	-0.4061

Table 2.4 (Continued): Out-of-Sample Forecasting Performance in Rolling Windows

70	2013-10-08	2017-09-26	2017-09-27	2019-09-25	0.2331	0.2105	-0.0226	-1.023
71	2013-12-18	2017-12-06	2017-12-07	2019-12-06	0.2413	0.2376	-0.0037	-0.1744
72	2014-03-04	2018-02-20	2018-02-21	2020-02-21	0.1673	0.1466	-0.0208	-1.851
73	2014-05-14	2018-05-02	2018-05-03	2020-05-05	2.3165	2.631	0.3142	1.086
74	2014-07-25	2018-07-13	2018-07-16	2020-07-17	2.3972	2.348	-0.0495	-0.2163
75	2014-10-06	2018-09-25	2018-09-26	2020-10-01	2.4769	2.471	-0.0057	-0.0362
76	2014-12-16	2018-12-05	2018-12-07	2020-12-11	2.3425	2.558	0.2150	1.979
77	2015-03-02	2019-02-20	2019-02-21	2021-02-26	2.2818	2.608	0.3257	2.359
78	2015-05-12	2019-05-02	2019-05-03	2021-05-10	2.3349	2.830	0.4952	1.214
79	2015-07-23	2019-07-16	2019-07-17	2021-07-21	2.3539	2.600	0.2458	1.224

2.6 Conclusion

We include another type of volatility - the VIX index - into the Realized GARCH model, and this new approach is called Realized GARCH-VIX model. We apply our model to the S&P 500 index, estimating and forecasting the actual volatility. By comparing the results with the benchmark Realized Volatility model, it shows that our model outperforms the benchmark model in volatility forecast due to a lower loss function. We also test the robustness of our results by conducting the rolling window analysis, and the results from rolling windows show that for most of the window, our model outperforms in the volatility forecast, and in addition, 24 out of 79 windows are statistically better than the benchmark model at a 10% significant level, using the Diebold-Mariano test method.

CHAPTER

3

US MONETARY SHOCK AND SPILLOVER EFFECT IN STOCK MARKET BETWEEN COUNTRIES

3.1 Introduction

Integration and interdependence between financial markets is a topic that has attracted much interest and generated considerable work in this area. The co-movement of world economic indices and stocks has been addressed by Panton et al. (1976), Ripley (1973), and Robichek et al. (1972), among others. Some studies have moved a step further, such as Hilliard (1979), Errunza and Losq (1985), and Malliaris and Urrutia (1992), which focus on the degree of

interdependence and causality between global stock markets.

The spillover effects in return and volatility between stocks or indices has been an issue that has attracted a lot of attention on stock interdependence. Generally, scholars study the spillover effect using two families of modeling methods - the family of VAR models and the family of GARCH models.

Substantial work on the spillover effect among stock markets is done with VAR models. Eun and Shim (1989) traces out the dynamic market responses of one stock market to innovations in another market by analyzing the daily data of nine major global stock markets in a VAR model and finds that the innovations in the US market have a rapid transmission to other countries. Jeon and Furstenberg (1990) tracks the impulse response functions of a VAR model, including the major global stock markets from January 1986 to November 1988, and the results show that the degree of co-movement increased significantly after the market crash in October 1987. Mathur and Subrahmanyam (1990) applies the "Granger Causality" concept to the VAR model and found that the US stock market affected only the Danish market but not the Norwegian, Finnish, or Swedish market.

Since volatility spillover has prominent time-varying characteristics (e.g., Schwert (1989)), the VAR model cannot accurately describe the volatility spillover effect. Thus, most scholars have recently examined the volatility spillover by adopting the family of GARCH models. Liu and Pan (1997) investigates the mean return and volatility spillover effects from the US and Japan to four Asian stock markets, including Hong Kong, Singapore, Taiwan, and Thailand, through the ARMA-GARCH model. They employed a two-stage GARCH approach - the first stage is modeling an ARMA-GARCH(1,1) model, and the second stage is to estimate the return and volatility spillover by obtaining the standardized residual and its square in the first stage and substituting them into the return and volatility equations - and they found that the US market is more influential than the Japanese market in transmitting returns and volatility to these four Asian markets. Miyakoshi (2003) used the EGARCH model to examine the extent of the return and volatility spillovers from Japan and the US to seven Asian equity markets.

However, they concluded that the volatility of Asian markets is influenced more by the Japanese stock market than the US stock market. Hahm (2004), on the other hand, established strong evidence of volatility spillover from the Korean market to the US market, while there is no significant supporting evidence for the reverse. Moon and Yu (2010) analyzed the short-term mean and volatility spillover between S&P 500 index and the Shanghai stock exchange index, and Nishimura and Men (2010) studied the over-night spillover effect of stock prices between China and G5 countries, respectively. Kundu and Sarkar (2016) used the TGARCH-M model to study the return and volatility spillover effects under two different market conditions - rising and falling markets. Liu (2016) compared the spillover effect between other model frameworks - the VAR approach and the GARCH BEKK model, and the results show that for the GARCH BEKK model, the impact of shocks from the US market is more substantial during the post-crisis (the 2008 financial crisis) era. Panda et al. (2019) also explored the short-term and long-term spillover effects under different model families.

Recently, Diebold and Yilmaz (2009), Diebold and Yilmaz (2012), Diebold and Yilmaz (2014) introduced a new methodology called connectedness network, which can be used to measure the total and directional pairwise spillover in a system. This method is not only applied in the research on spillover effect in financial markets (see Abuzayed et al. (2021), Youssef et al. (2021), Arif et al. (2021), Akhtaruzzaman et al. (2021), etc.), but also in the research on the spillover effect in the commodity markets, futures markets and among other markets (such as interdependence between energy and stock markets). Many articles have contributed to this topic (see Antonakakis et al. (2017), Song et al. (2019), Zhang and Hamori (2021), Bouri et al. (2021), Saeed et al. (2021), etc.). Moreover, Diebold and Yilmaz (2014) claimed that connectedness could be applied to other areas, such as portfolio management and policy. Thus, much work still needs to be done in this research area. Unfortunately, little work has focused on the connectedness between assets and policy shocks.

In this paper, we try to establish the connectedness between the global stock market and an endogenous shock - US monetary policy shock, and investigate the interdependence between

the stock market evolution and this US economic shock.

The rest of this chapter is organized as follows: Section 2 introduces the Federal Funds rate and the global influence of the US monetary policy; Section 3 provides the methodology of our analysis; Section 4 illustrates the data from representative stock markets and discusses the empirical results of our framework; Section 5 tests the robustness of the connectedness network; and Section 6 concludes this article and proposes possible future researches.

3.2 Federal Funds Rate and the US Monetary Shock

The Federal Funds rate is the interest rate at which depository institutions (banks and credit unions) lend reserve balances to each other overnight. It serves as a benchmark for short-term interest rates and influences borrowing costs across the broader economy. The Federal Funds rate target is an internal objective that is set by the chairman of the Federal Reserve System (the Fed) in compliance with the directives agreed on at meetings of the Federal Open Market Committee (FOMC). The target is used by the trading desk of the Federal Reserve Bank of New York as a guide for the daily conduct of open market operations. It is of much interest to the economy since it is an indicator of the determination of the direction of the monetary policy.

There have been other tools for the Fed to influence monetary policy, such as buying large amounts of government securities. However, the Fed has intended to regard the Federal Funds rate as a more important policy tool since the end of 2008. For example, according to "The Federal Reserve System Purposes & Functions - Section 3", in December 2015, the FOMC decided that economic conditions and the economic outlook warranted starting the process of policy normalization and voted to raise its target for the Federal Funds rate. Thus today we often refer to the changes in the Federal Funds rate target as the adjustment of the monetary policy.

The monetary policy will influence the economy in many aspects, such as the short-term and long-term interest rates, the inflation rate, stock prices, etc. Thus, the monetary policy

could be referred to as a shock in the economic system. The US monetary policy, in particular, could be regarded as a global shock since most of the international trade is traded in US dollars. Some scholars have noted this impact, for example, Kim (2001) found that an expansionary US monetary policy will lead to a decrease in the world interest rate and thus results in a boom in non-US, G6 countries; Ehrmann and Fratzscher (2009) analyzed the transmission of US monetary policy shocks to global equity markets and it shows that there is a substantial cross-country heterogeneity in reactions across 50 equity markets worldwide; Laeven and Tong (2012) studied the global stock price responses to the US monetary policy and interest rate; Miranda-Agrippino and Rey (2020) pointed out that the US monetary shocks induce co-movements in the international financial markets and characterize a "Global Financial Cycle".

Accordingly, the Federal Funds rate will influence not only the US stock market, but also the interest rate and financial markets worldwide. Thus it can be regarded as a global endogenous shock variable when we analyze the spillover over effect between international stock markets.

3.3 Model and Methodology

We construct a VAR model:

$$\begin{pmatrix} y_{1t} \\ y_{2t} \\ y_{3t} \\ y_{4t} \\ \vdots \\ shock_t \end{pmatrix} = \begin{pmatrix} \omega_1 \\ \omega_2 \\ \omega_3 \\ \omega_4 \\ \vdots \\ shock_0 \end{pmatrix} + \sum_{i=1}^p A_i \begin{pmatrix} y_{1,t-i} \\ y_{2,t-i} \\ y_{3,t-i} \\ y_{4,t-i} \\ \vdots \\ shock_{t-i} \end{pmatrix} + \epsilon_t \quad (3.1)$$

The variable $shock_t$ represents a policy (or endogenous) shock within the economic system, and it denotes the US monetary shock in our paper; the error term ϵ_t denotes the exogenous

shock.

To study the spillover effect, we apply the connectedness network method introduced by Diebold and Yilmaz (2014). The VAR model

$$y_t = \omega + \sum_{i=1}^p A_i y_{t-i} + \epsilon_t \quad (3.2)$$

can be rewritten as the MA (moving-average) form, assuming it is stationary:

$$y_t = \mu + \sum_{j=0}^{\infty} \psi_j \epsilon_{t-j} \quad (3.3)$$

where $\mu = (I - \sum_{i=1}^p A_i)^{-1} \omega$, $\psi_j = \sum_{l=1}^p A_l \psi_{j-l}$, and ψ_0 is an $N \times N$ identity matrix.

In Eq. 3.3, the moving average coefficient represents the effects of a specific shock over a future period. According to the generalized variance decomposition method proposed by Pesaran and Shin (1998), the H -step-ahead generalized forecast error variance of variable i due to the shock in variable j is defined by:

$$\theta_{ij}^H = \frac{\sigma_{jj}^{-1} \sum_{h=0}^{H-1} (e_i' \psi_h \Sigma e_j)^2}{\sum_{h=0}^{H-1} (e_i' \psi_h \Sigma \psi_h' e_i)^2}, \quad (3.4)$$

where ψ_h denotes the h th coefficient matrix of the moving average process derived from the above VAR model in Eq. 3.2, Σ denotes the covariance matrix for the shock vector ϵ_t , σ_{jj} represents the j th diagonal element of Σ , and e_j is an $N \times 1$ selection vector with the value one for j th element and zero for otherwise. According to this definition, θ_{ij} includes the information on the proportion of the H -step-ahead forecast error for variable i that the shocks in variable j can explain. Since the sums are not necessarily equal to unity, θ_{ij}^H in Eq. 3.4 could further be normalized as:

$$\tilde{\theta}_{ij}^H = \frac{\theta_{ij}^H}{\sum_{j=1}^N \theta_{ij}^H} \quad (3.5)$$

where N denotes the number of variables. After normalization, we know that by definition,

$$\sum_{j=1}^N \tilde{\theta}_{ij}^H = 1.$$

According to Diebold and Yilmaz (2014), in a connectedness network, the pairwise directional connectedness from variable j to i can be defined as follows:

$$C_{i \leftarrow j}^H = \tilde{\theta}_{ij}^H \quad (3.6)$$

Note that $C_{i \leftarrow j}^H \neq C_{j \leftarrow i}^H$, thus there are $N^2 - N$ measurements of pairwise directional spillover effects. Then the net directional spillover effect of variable j from variable i is $C_{ij}^H = C_{j \leftarrow i}^H - C_{i \leftarrow j}^H$, and there are $(N^2 - N)/2$ measurements of net pairwise directional spillover effect.

In addition, the spillover effect of variable i from the system (or can be called "From Spillover" in short) could be defined as:

$$C_{i \leftarrow \bullet} = \sum_{j=1, j \neq i}^N \tilde{\theta}_{ij}^H \quad (3.7)$$

and the directional spillover of variable j to the system (or can be called "To Spillover" in short) is defined as:

$$C_{\bullet \leftarrow j} = \sum_{i=1, i \neq j}^N \tilde{\theta}_{ij}^H \quad (3.8)$$

Thus the net spillover of variable j to the system could be written as:

$$C_{\bullet \leftarrow j}^{Net} = C_{\bullet \leftarrow j} - C_{j \leftarrow \bullet} \quad (3.9)$$

Then there are $2N$ measurements for the total directional spillover effect (both "To" and "From" spillover). And the total spillover effect of the system is defined as:

$$C^H = \frac{1}{N} \sum_{i, j=1, i \neq j} \tilde{\theta}_{ij}^H \quad (3.10)$$

The total spillover index measures the explanatory ability of variables in the system. Thus there is only one measurement.

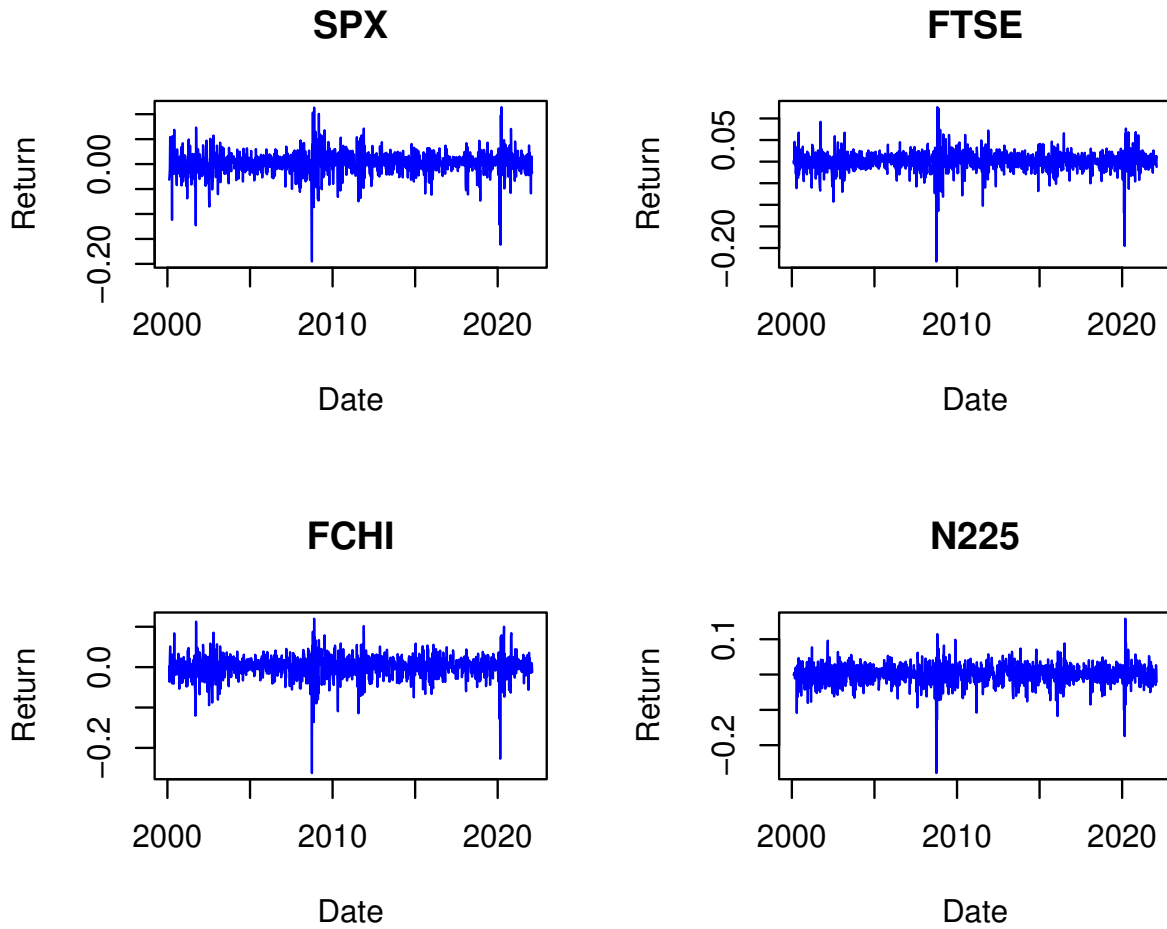
Since the VAR model is a reduced form, we do not impose a structural effect on the model. When we re-order the series, the values in the matrices Σ and ψ_h don't change, they just change places. As a result, we have to get the same θ_{ij}^H (after keeping track of what i and j represent after the re-ordering). Therefore, connectedness results are not dependent on the ordering of the series and this is not problematic because the method is not trying to capture the impact of structural shocks.

3.4 Empirical Results

We take the realized library of the Oxford-Man Institute of Quantitative Finance from Jan 1, 2000, to Feb 18, 2022, as our data set. To study the spillover effect of the global financial market, we select the S&P 500 index (denoted as SPX in tables) to represent the US stock market, the FTSE 100 index (denoted as FTSE) as the UK stock market, the CAC 40 index (denoted as FCHI) as the French stock market, and the Nikkei 225 index (denoted as N225) as the Asian stock market. Since the US monetary shock will affect the global stock market, we select the Federal Funds rate as the "global shock" variable.

Due to the time difference between those countries, there is a structural effect on the daily data. For example, the open time of the CAC 40 index is 6 hours earlier than the S&P 500 index, and thus the French market has an effect on today's US market, but the US market could not affect the French market on the same day. We use weekly data instead of daily data to eliminate these structural effects. The weekly data for the Federal Funds rate is taken as the average effective Federal Funds rate of the week, the weekly return is defined by the difference of the log-close-price for the last weekday of two consecutive weeks, and the weekly realized volatility is the sum of the daily volatility and the overnight volatility (squared returns) during a week. We get 1147 valid weekly observations for those variables. The plots of these weekly data series are shown in Figure 3.1, 3.2 and 3.3.

Figure 3.1: Weekly Return Series

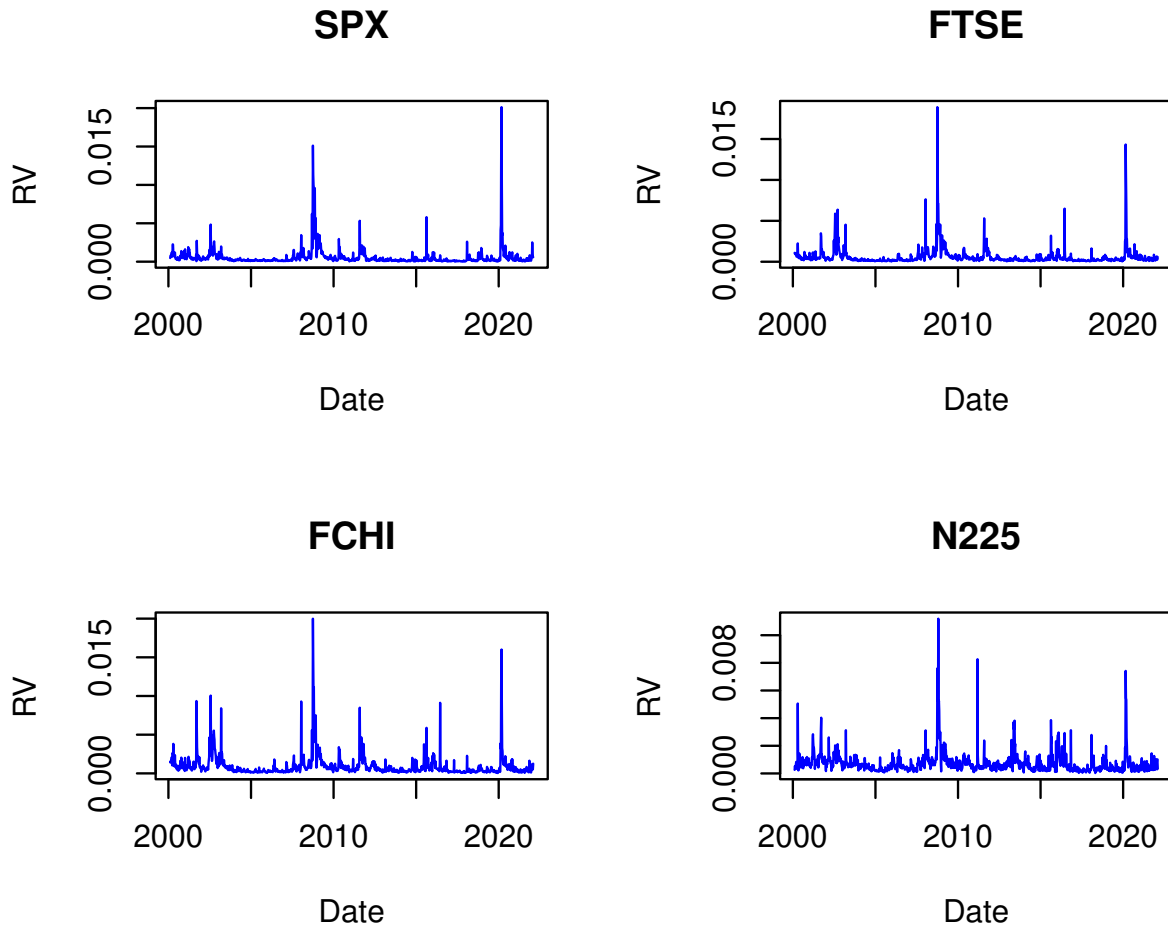


3.4.1 Return System Spillover

Here we first study the spillover effect of the return system for the whole sample from Jan 2000 to Feb 2022. By applying AIC to our VAR model, the optimal lags are 7 and 3 for the return system, with and without incorporating the Federal Funds rate, respectively. Tables 3.1 and 3.2 show the spillover effect of the return system, without and with including the Federal Funds rate, respectively.

Starting with the system without the Federal Funds rate, let us look at the diagonal elements in Table 3.1 and explain their economic intuition. The total spillover index, C^H , of the return

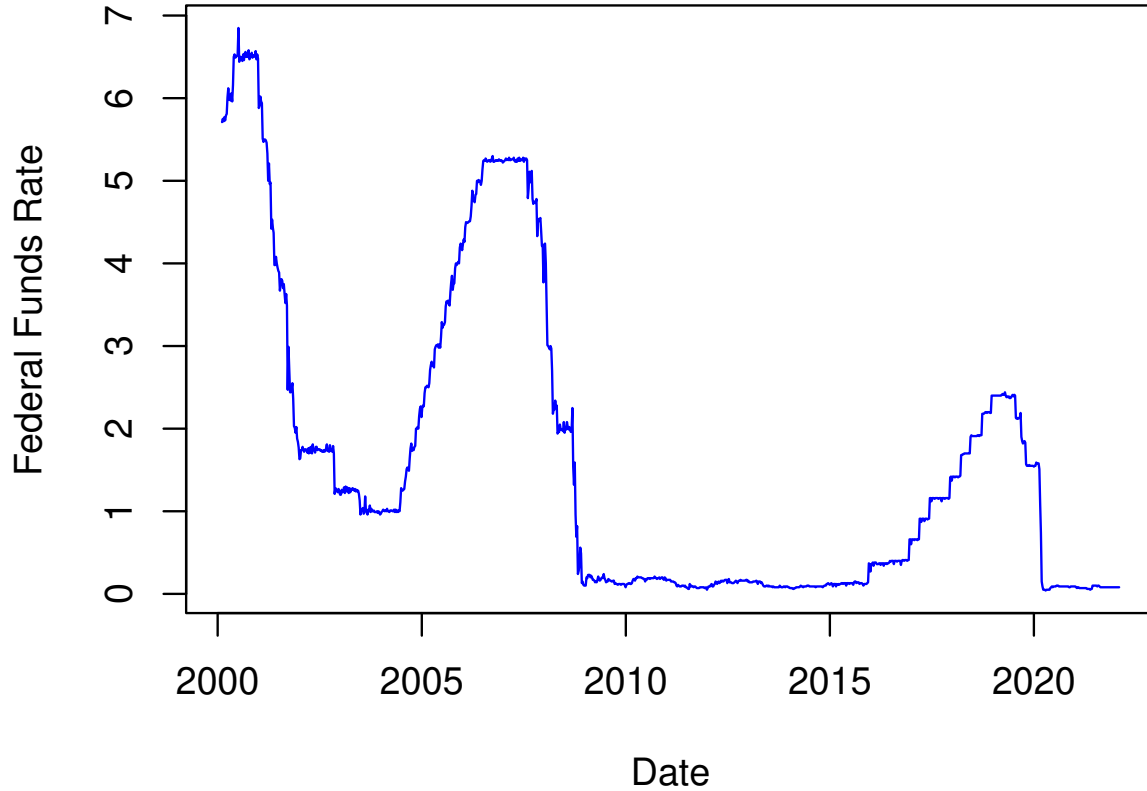
Figure 3.2: Weekly Volatility Series



system is 61.36%, which means that about 3/5 of the variations in the stock indices in the return system are caused by the interactions among them. The values of the rest of the diagonal items measure the forecast error variance caused by itself for each of them. A greater value indicates that the single stock market is largely affected by itself, rather than the system. In other words, it is more “independent” from the system. This value for the Nikkei 225 index is the greatest among all indices (46% compared with less than 40% for other indices), thus the Japanese stock market is relatively less connected to the European and US stock markets.

We further discuss the features of the connectedness table by discussing the pairwise directional connectedness measures, which are the off-diagonal elements, $C_{i \leftarrow j}^H$. Note that

Figure 3.3: Weekly Federal Funds Rate Series



the table is not symmetric, for example, the spillover from the FTSE 100 index to the S&P 500 index ($C_{SPX \leftarrow FTSE}^H$) is 24.53%, compared with the value of 22.98% for the opposite direction ($C_{FTSE \leftarrow SPX}^H$). Therefore, we could say that in this 20-year span, the FTSE 100 index has a positive net spillover effect on the S&P 500 index, though the value of 1.55% is not quite significant. By comparing the corresponding off-diagonal elements, we can learn that the FTSE 100 and the CAC 40 index have net impacts on the S&P 500 index, while all other stock indices have a net impact on the Japanese stock market. Moreover, the value of the off-diagonal elements for the Nikkei 225 index are relatively smaller than those between European and US stock markets, and it is consistent with the intuition we discussed above, i.e., the Japanese market is

Table 3.1: Whole Sample Return Connectedness without Federal Funds Rate

To (i) / From (j)	SPX	FTSE	FCHI	N225	From ($C_{i\leftarrow\bullet}$)
SPX	38.02	24.53	23.94	13.50	15.49
FTSE	22.98	35.55	28.31	13.15	16.11
FCHI	22.35	28.14	34.97	14.54	16.26
N225	17.14	17.37	19.49	46.00	13.50
To ($C_{\bullet\leftarrow j}$)	15.62	17.51	17.94	10.30	61.36 (Total C^H)
Net ($C_{\bullet\leftarrow j}^{Net}$)	0.13	1.40	1.68	-3.20	

Return Connectedness Table without Federal Funds rate for the whole sample. The values are percentage values, i.e., true value scaled by 100. The predictive horizon is four weeks ahead. The ij -th entry of the upper-left 4×4 index sub-matrix gives the ij -th pairwise directional connectedness, i.e., the percent of 4-week-ahead forecast error variance of variable i due to shocks from variable j . The rightmost (From) column gives total directional connectedness (from), i.e., row sums (from all others to i). The bottom (To) row gives total directional connectedness (to), i.e., column sums (to all others from j). The most bottom (NET) row gives the difference in total directional connectedness (to–from). The bottom-right element is total connectedness (mean “from” connectedness, or equivalently, mean “to” connectedness).

less connected to the European and US stock markets.

Finally, we look at the system spillovers, “To” ($C_{\bullet\leftarrow j}$) and “From” ($C_{i\leftarrow\bullet}$) spillovers. The “To” spillover measures the contribution to the system of each variable. For example, the CAC 40 index has the greatest contribution to the system (17.94%), among the total system spillover of 61.36%. Whereas the Nikkei 225 index has the smallest contribution, only about 10%, to the return system. On the other hand, the “From” spillover measures the variation of one stock market influenced by other variables. In the return system, the differences in the “From” spillovers between different stock markets are not significant, from the lowest value of 13.50% for the Japanese market to the highest value of 16.26% for the French market. The sums of both the “To” and “From” spillovers are equal to the total spillover index. The net directional spillover of each variable ($C_{\bullet\leftarrow j}^{Net}$), which is the last row of the table, is the difference between the

Table 3.2: Whole Sample Return Connectedness with Federal Funds Rate

To (i) / From (j)	FFR	SPX	FTSE	FCHI	N225	From ($C_{i \leftarrow \bullet}$)
FFR	75.90	4.82	8.68	6.47	4.13	4.82
SPX	0.86	37.80	24.25	23.94	13.15	12.44
FTSE	0.60	22.92	35.38	28.16	12.94	12.92
FCHI	0.58	22.43	27.91	34.70	14.37	13.06
N225	0.82	17.02	17.18	19.36	45.62	10.88
To ($C_{\bullet \leftarrow j}$)	0.57	13.44	15.60	15.59	8.92	54.12 (Total C^H)
Net ($C_{\bullet \leftarrow j}^{Net}$)	-4.25	1.00	2.68	2.53	-1.96	

Return Connectedness Table with Federal Funds rate for the whole sample. 4-week-ahead variance forecast.

“To” and “From” spillover. The US and European stock markets have a positive net directional total spillover (0.13% for S&P 500, 1.40% for FTSE 100, and 1.68% for CAC 40 index, respectively), which means that they are the net information contributor to the return system. The result is the opposite for the Nikkei 225 index, who has a negative net spillover (-3.20%), which implies that the Japanese market is the net information receiver from the system.

We next study the results in table 3.2, which shows the results of the return system when we include the Federal Funds rate. First, the self-spillover of the Federal Funds rate ($C_{FFR \leftarrow FFR}^H$) is quite large (75.9%), which means that less than 1/4 of the variation in the Federal Funds rate is caused by the global stock markets in the return system. It implies that the US monetary policy is not largely affected by the stock market returns behavior during this 20-year period. Second, the corresponding items in Table 3.2, including the directional pairwise connectedness, and “To” and “From” spillovers, are quite similar to those in Table 3.1. This is due to the directional pairwise connectedness from the Federal Funds rate to the stock markets being quite insignificant, less than 1% for all markets. On the other hand, the pairwise directional spillovers from the stock markets to the Federal Funds rate are greater than the opposite, which indicates that the stock markets have positive net impacts on the US monetary policy, while the stock markets are not influenced by the Federal Funds rate. Thus the net total spillover from the Federal Funds rate ($C_{\bullet \leftarrow FFR}^{Net}$) is negative (-4.25%). In addition, the value of the total

spillover index of the return system decreases to 54.12% when we include the Federal Funds rate in our model, because the Federal Funds rate is relatively independent in the return system. Accordingly, the US monetary policy does not contribute much to the variations in the return system and is a net information receiver.

3.4.2 Volatility System Spillover

Table 3.3: Whole Sample Volatility Connectedness without Federal Funds Rate

To (i) / From (j)	SPX	FTSE	FCHI	N225	From ($C_{i \leftarrow \bullet}$)
SPX	38.62	26.81	23.23	11.34	15.34
FTSE	27.62	33.14	28.21	11.03	16.71
FCHI	26.50	30.02	32.09	11.39	16.98
N225	22.14	21.38	20.49	35.99	16.00
To ($C_{\bullet \leftarrow j}$)	19.07	19.55	17.98	8.44	65.04 (Total C^H)
Net ($C_{\bullet \leftarrow j}^{Net}$)	3.73	2.84	1.00	-7.56	

Volatility Connectedness Table without Federal Funds rate for the whole sample. 4-week-ahead forecast

Table 3.4: Whole Sample Volatility Connectedness with Federal Funds Rate

To (i) / From (j)	FFR	SPX	FTSE	FCHI	N225	From ($C_{i \leftarrow \bullet}$)
FFR	47.83	15.42	15.18	14.84	6.73	10.43
SPX	0.56	37.95	26.81	23.12	11.55	12.41
FTSE	0.45	27.54	32.90	28.06	11.05	13.42
FCHI	0.22	26.46	29.93	31.89	11.50	13.62
N225	0.31	22.22	21.21	20.48	35.79	12.84
To ($C_{\bullet \leftarrow j}$)	0.31	18.33	18.63	17.30	8.17	62.73 (Total C^H)
Net ($C_{\bullet \leftarrow j}^{Net}$)	-10.12	5.92	5.21	3.68	-4.67	

Volatility Connectedness Table with Federal Funds rate for the whole sample. 4-week-ahead variance forecast.

After summarizing the results for the return system, now we look at what happens in the volatility system during the 20-year period. By applying AIC to the VAR model for the volatility system, the optimal lags are 9 and 7 with and without including the Federal Funds rate in the volatility system, respectively.

The volatility system spillover results without the Federal Funds rate are shown in Table 3.3. Let us first look at the diagonal items of this table. The total spillover index of the volatility system is 65.04%, which is slightly greater than the value of 61.36% in the return system. Therefore, there are more interactions between stock volatility than between returns. The values of the rest of the diagonal elements are quite similar to each other, from the minimum value of 32.09% for the CAC 40 index to the maximum value of 38.62 for the S&P 500 index. All the corresponding values are close to those in the return system, except for the value of the Nikkei 225 index, which is 35.99% and is significantly lower than 46.00% in the return system. It indicates that the volatility in the Japanese market is more connected with the world stock market than for the returns. Thus unlike the return system, there is no stock market that is significantly more independent in the volatility system.

Next, we move to the off-diagonal elements which represent the pairwise directional spillover effect. By comparing the off-diagonal values between the S&P 500 index and all other stock indices, we learned that in the volatility system, the US stock market has a greater directional spillover to other stock markets than the opposite direction. In other words, the S&P 500 index has a positive net spillover effect on all other indices, while it is a different story for the FTSE 100 index and CAC 40 index in the return system. Besides, the pairwise spillover indices are about 11% from the Nikkei 225 index to other markets, which is a small decrease compared to the return system (about 13% to 14%). On the contrary, the pairwise directional spillover from other stock markets to the Japanese market increases a bit (about 21% to 22%) compared with the return system (about 17% to 19%). This explains why the value of the diagonal element for the Nikkei 225 index shrinks in the volatility system.

Finally, we look at the results of system spillovers, "To" and "From" spillovers. The FTSE 100

index has the greatest contribution to the volatility system (19.55% of 65.04% total), compared with the lowest contribution from the Nikkei 225 index (only 8.44%). On the other hand, like in the return system, there is no significant difference in the "From" spillover between different stock markets, with values around 15% - 17%. Moreover, the net directional total spillover in the volatility system is similar to the return system. The European and US stock markets have a positive net contribution to the system (3.73% for the S&P 500 index, 2.84% for the FTSE 100 index, and 1.00% for the CAC 40 index), while the Japanese stock market has a negative net contribution (-7.56%), which is even a greater value than in the return system.

We next discuss the results in Table 3.4, which shows the results of the volatility system including the Federal Funds rate. First, the value of the diagonal element for the Federal Funds rate (47.83%) is still the greatest value among all the variables, which means that about half of the variation in the Federal Funds rate is caused by the volatility in global stock markets. However, this value is significantly smaller than that in the return system (75.90%). It suggests that the US monetary policy is more influenced by global stock volatility than the returns. Thus the value of the total spillover index in the volatility system does not decrease greatly after we include the Federal Funds rate (62.73% compared with 65.04% in Table 3.3). Secondly, the values of the corresponding elements in Table 3.4, including the pairwise directional spillover and the "To" spillover, are very close to those in Table 3.3. This result is similar to the return system, i.e., there are few directional spillover effects from the Federal Funds rate to global stock markets. On the opposite direction, the global stock markets have significant directional spillover to the Federal Funds rate, from 6.73% for the Nikkei 225 index to 15.42% for the S&P 500 index. These values are much larger than those in the return system. Thus the "From" spillover for the Federal Funds rate is also greater in the volatility system (10.43%). In other words, global stock volatility has an even greater impact on the US monetary policy. As a result, the net contribution of the Federal Funds rate is a quite negative number -10.12%, while by contrast, the net contributions from other variables increase to some extent compared with the values in Table 3.3. So in general, we could say that the US monetary policy does not contribute

much to the variations in global stock market volatility, and it is greatly influenced by stock volatility.

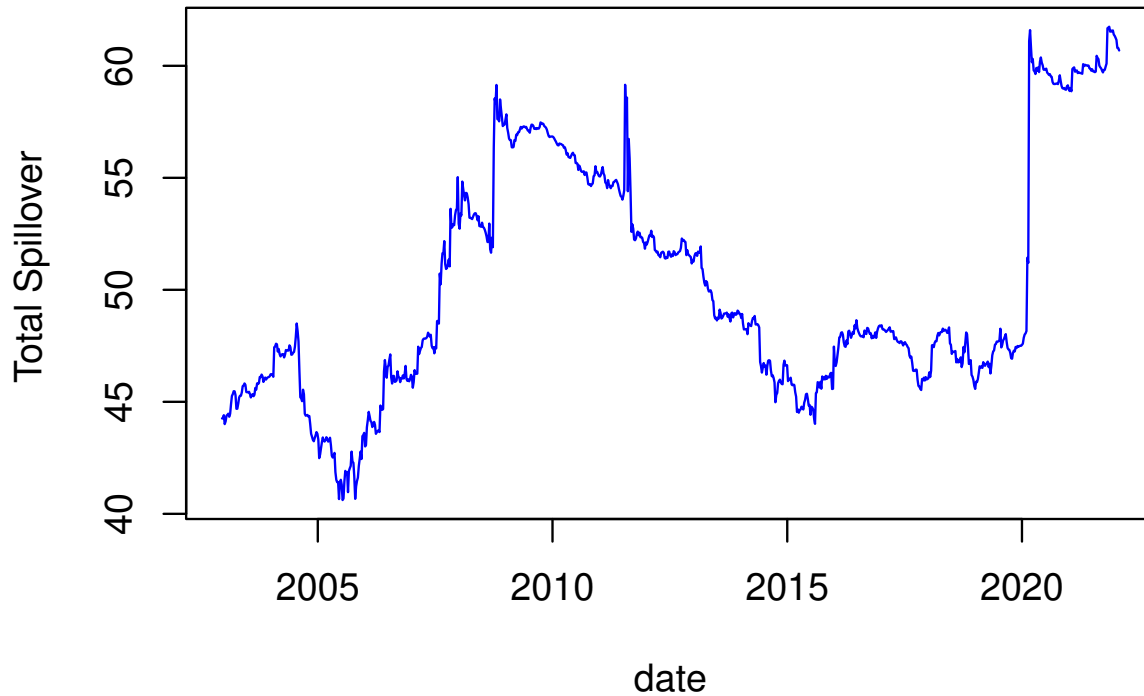
3.4.3 Rolling Window Analysis

In this section, we investigate the spillover effect in a shorter scope to examine the contribution of the Federal Funds rate to the system in a shorter or a particular period. The interdependence between global stock market returns and volatility could vary a lot among different short periods. For example, Jeon and Furstenberg (1990) found that the co-movement between global stock markets reaches a higher degree right after the 1987 market crash. Besides, Diebold and Yilmaz (2014) also investigate the dynamics of the connectedness network between 13 firm stocks from the year 1999 to 2010, and it suggests that the total spillover index is higher during the 2008 financial crisis than any other period. Thus it is interesting to do a rolling window analysis and see if there are any differences in the spillover effects during different short-term periods.

Now we screen the rolling window (with 150 observations per window, about three years) to see how the spillover effects in the return and volatility system change over time.

Let's first look at the dynamic of total spillover in rolling windows for the return and volatility system (see Fig. 3.4 and 3.5). The figures describe the dynamic of total spillover with including the Federal Funds rate. For the return system, the total spillover index ranges from about 40% to 61%, and the average value is about 50%, close to the full-sample average value of 54.12%. We could see a significant increase in the total spillover index after the 2008 financial crisis, and then a decrease after the year 2012. It again meets a rapid increase in the year 2020, after the outbreak of the COVID-19 pandemic, and the value is even greater than that during the 2008 financial crisis. The story of the total spillover index in the volatility system is almost the same. It reaches its high point during the 2008 financial crisis, then decreases after the year 2012, and again jumps to the highest point after the outbreak of the COVID-19 pandemic. The range of the total spillover in the volatility system is larger, from lower than 40% to around 80%.

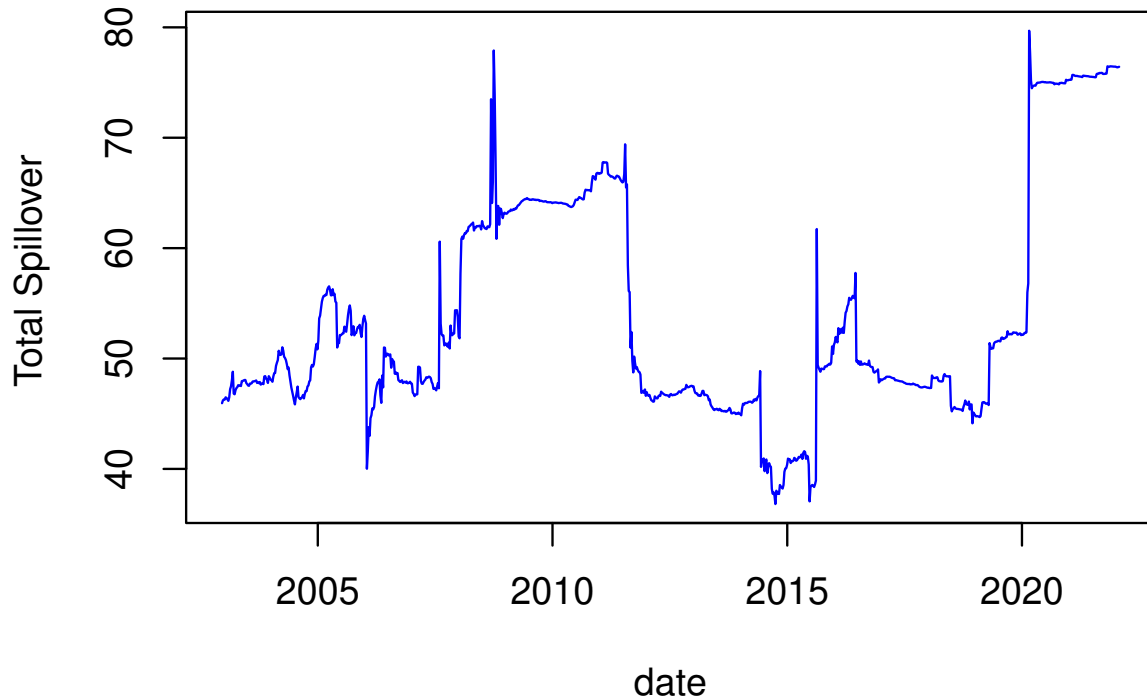
Figure 3.4: Dynamics of Total Spillover in Return System



Next, we look at the dynamics of the “To Spillover” for each variable in rolling windows for both the return and volatility systems.

Fig. 3.6 shows each variable’s total spillover to the return system. The spillover from the Federal Funds rate to the system does not significantly change over time, only a range from 0.0% to 1.5%. However, we could still see some jumps (around 2008, 2012, 2016, and 2020) over the past 20 years. The contribution from the S&P 500 index has a cyclical pattern over the rolling windows. It reached its highest point around 2005 and then decreased, again increasing around the beginning of the 2008 financial crisis and remaining high until 2015, then growing again around 2020 when the COVID pandemic became a global issue. The contribution from Nikkei 225 index has a similar pattern as the S&P 500 index. The pattern of the FTSE 100 index

Figure 3.5: Dynamics of Total Spillover in Volatility System



remained almost unchanged from the year 2003 to the year 2016, then had a significant jump around 2020, when COVID began. Besides, the CAC 40 index has a similar pattern to the FTSE 100 index concerning the dynamics of the “To Spillover”.

Fig. 3.7 shows the dynamics of the “To Spillover” from each variable in the volatility system. In the volatility system, the spillover from the Federal Funds rate to the system changed significantly over time, with a range going from 0.0% to about 15%, and it underwent a rapid increase in the year 2008 and 2012, after which a rapid decrease occurred. The “To Spillover” for the S&P 500 index in the volatility system has a similar pattern as the return system, i.e., a cyclical pattern with high points at around 2005, 2008, and 2020, along with low points at about 2006 and 2016. The impact on the system from Nikkei 225 index also has a cyclical pattern.

However, it encounters a rapid decrease at the beginning of the year 2020, which is different from the pattern in the return system. The dynamic patterns for the FTSE 100 index and the CAC 40 index are similar to the patterns in the return system - the "To Spillover" did not have a significant change before the year 2020 and then encountered a considerable jump when the COVID pandemic caused a great panic across the world.

According to our rolling window analysis, it is worth investigating the spillover effect during extraordinary periods, i.e., the 2008 financial crisis and after the COVID outbreak, when the stock markets highly interacted with each other. Since the causalities of the two crises are different - the 2008 financial crisis resulted from the internal shock of the economic system, while the crisis after 2020 is primarily caused by external uncertainty - we could expect different results and intuitions between the two periods.

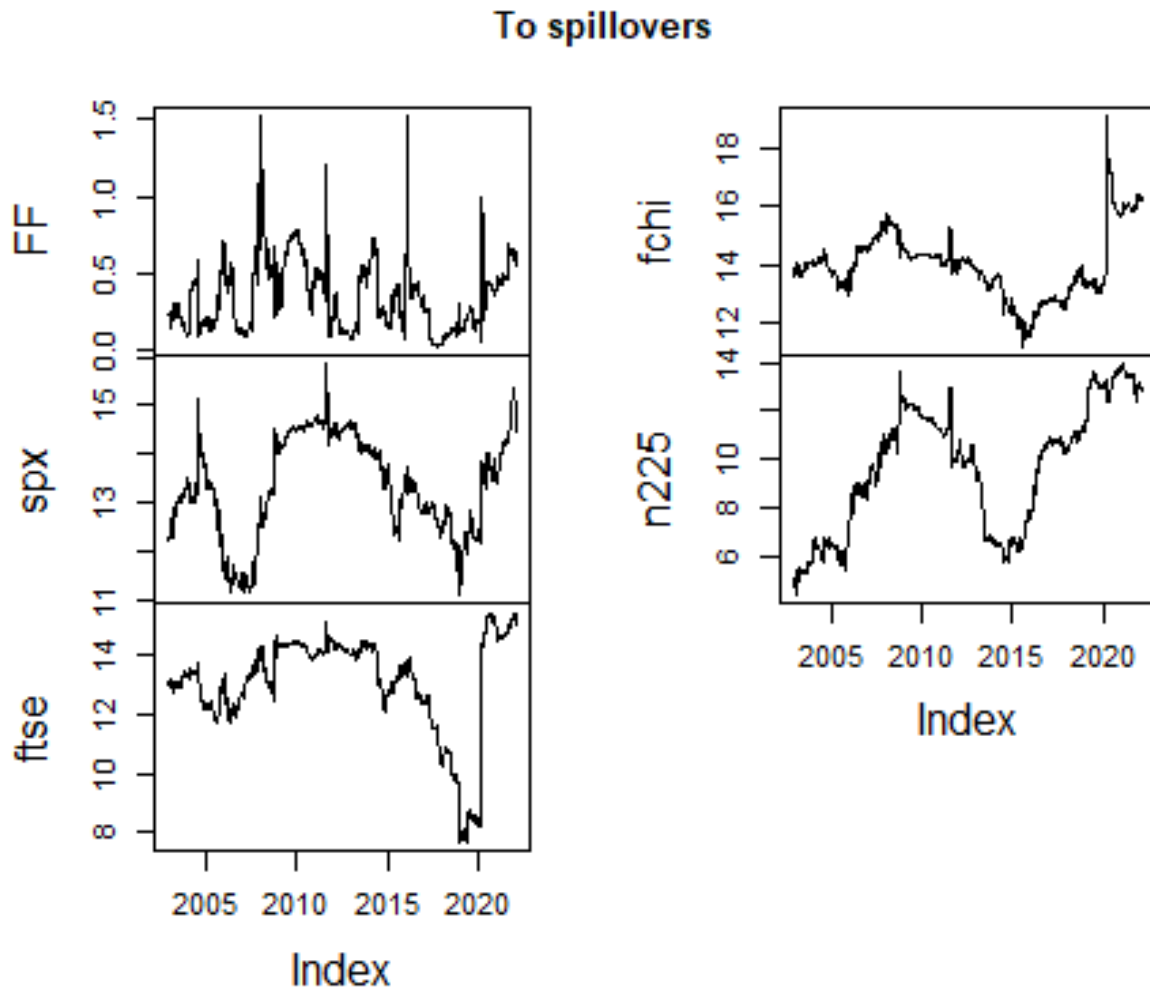
3.4.4 Spillover During the 2008 Financial Crisis

We pick the observations from Jan 2008 to March 2010 (a total of 113) to study the spillover effect during the 2008 financial crisis. This time period covers the crisis period in 2008, as well as the monetary policy reaction of the Federal Reserve after the crisis.

Return System

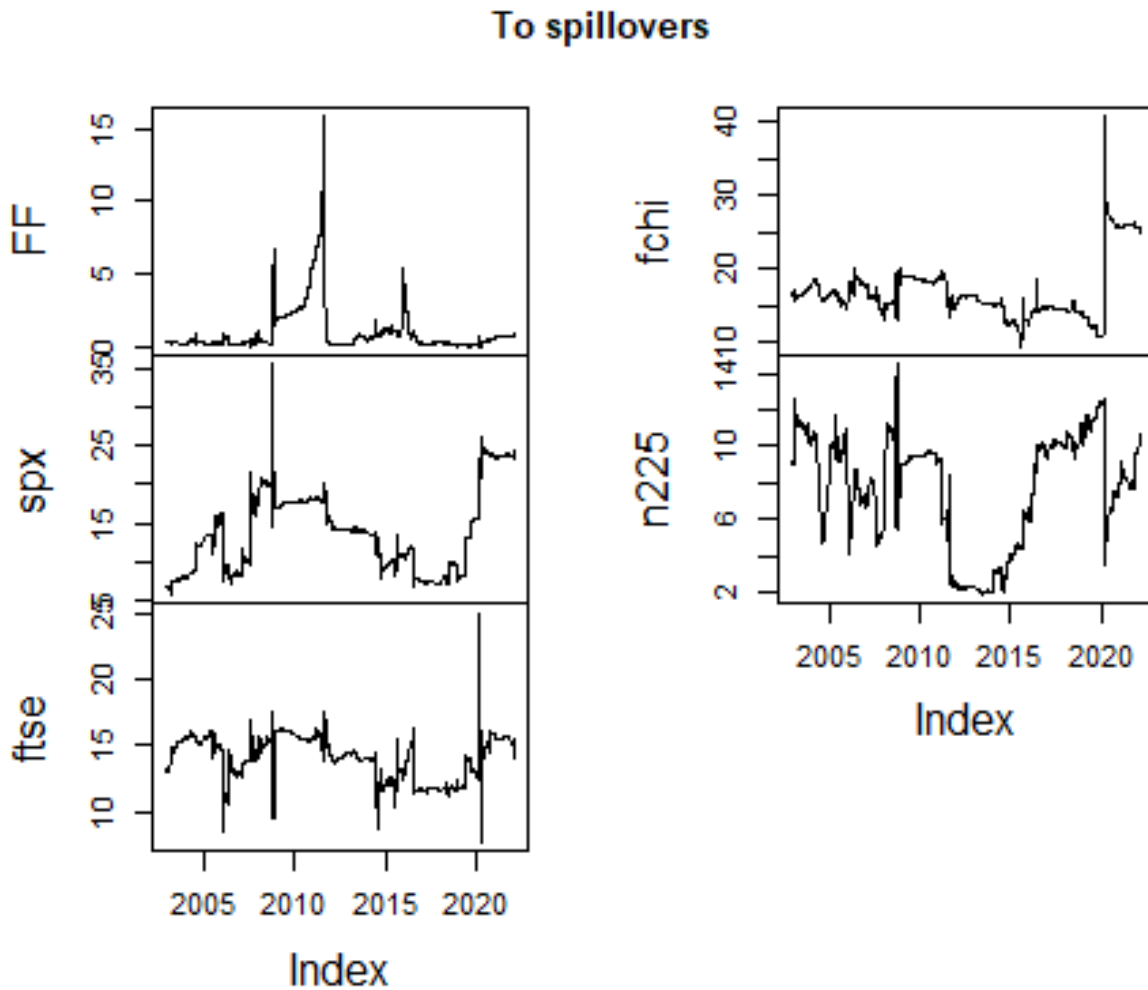
Tables 3.5 and 3.6 show the spillover effect of the return system during the 2008 financial crisis with and without including the Federal Funds rate in our model, respectively. The features of Table 3.5 are similar to those of Table 3.1, which describes the 20-year average spillover of the return system, and the main difference between them is a higher total spillover index (67.74% vs. 61.36%). Thus there is more connectedness between global stock markets during the 2008 financial crisis than in normal periods. Accordingly, the diagonal elements in Table 3.5 are lower than those in Table 3.1, especially for the Nikkei 225 index, whose self-spillover index decreases by nearly 10% (from 46% to 36.24%), while the off-diagonal elements are greater during the financial crisis.

Figure 3.6: Spillover to the Return System



We next discuss the results in Table 3.6, which summarizes the spillover of the return system during the 2008 financial crisis when we include the Federal Funds rate. First, the Federal Funds rate is quite independent from the return system during this period and the self-spillover index, $C_{FFR \leftarrow FFR}^H$, is 83.07%, which is even greater than the 75.90% for the full sample. And this results in a significant decrease in the total spillover effect index (58.17% compared with 67.74%) after we include the Federal Funds rate in our system, but the value is still greater than the 20-year value of 54.12%. Secondly, the corresponding values in Table 3.6 are very close to those in Table

Figure 3.7: Spillover to the Volatility System



3.5, and it is due to the pairwise directional spillover from the Federal Funds rate to the global stock markets being very insignificant in the return system (only about 1%), which is similar to the result for the 20-year whole sample in Table 3.1. On the other hand, the pairwise directional spillover from the stock markets to the Federal Funds rate is greater than the opposite. Thus during the financial crisis, the return system of the global stock market still has a positive net impact on the US monetary policy, and as a result, the “To spillover” for the Federal Funds rate is negative (-2.44%) in the return system.

The results of spillover in the return system during the 2008 financial crisis have no significant differences from the 20-year whole sample, and the primary difference is a decrease in the value of the diagonal elements and an increase in the value of the off-diagonal elements for the connectedness tables.

Table 3.5: Return Connectedness without FFR during 2008 Financial Crisis

To (<i>i</i>) / From (<i>j</i>)	SPX	FTSE	FCHI	N225	From ($C_{i \leftarrow \bullet}$)
SPX	31.87	25.19	24.59	18.34	17.03
FTSE	24.09	30.42	27.98	17.50	17.39
FCHI	23.47	27.94	30.49	18.10	17.38
N225	21.36	20.86	21.54	36.24	15.94
To ($C_{\bullet \leftarrow j}$)	17.23	18.50	18.53	13.49	67.74 (Total C^H)
Net ($C_{\bullet \leftarrow j}^{Net}$)	0.20	1.11	1.15	-2.45	

Return Connectedness Table without Federal Funds rate before and after 2008 financial crisis. 4-week-ahead forecast

Table 3.6: Return Connectedness with FFR during 2008 Financial Crisis

To (<i>i</i>) / From (<i>j</i>)	FFR	SPX	FTSE	FCHI	N225	From ($C_{i \leftarrow \bullet}$)
FFR	83.07	2.68	3.11	4.18	6.95	3.39
SPX	1.41	30.47	25.37	24.58	18.17	13.91
FTSE	1.18	23.81	30.12	27.66	17.24	13.98
FCHI	1.09	22.99	27.73	30.21	17.98	13.96
N225	1.08	20.88	21.08	21.67	35.29	12.94
To ($C_{\bullet \leftarrow j}$)	0.95	14.07	15.46	15.62	12.07	58.17 (Total C^H)
Net ($C_{\bullet \leftarrow j}^{Net}$)	-2.44	0.16	1.48	1.66	-0.87	

Return Connectedness Table with Federal Funds rate before and after 2008 financial crisis. 4-week-ahead forecast

Table 3.7: Volatility Connectedness without FFR during 2008 Financial Crisis

To (<i>i</i>) / From (<i>j</i>)	SPX	FTSE	FCHI	N225	From ($C_{i \leftarrow \bullet}$)
SPX	36.35	25.60	26.16	11.89	15.91
FTSE	36.24	25.62	26.51	11.62	18.59
FCHI	35.91	25.82	26.81	11.45	18.30
N225	33.53	26.57	26.54	13.35	21.66
To ($C_{\bullet \leftarrow j}$)	26.42	19.50	19.80	8.74	74.46 (Total C^H)
Net ($C_{\bullet \leftarrow j}^{Net}$)	10.51	0.91	1.5	-12.92	

Volatility Connectedness Table without Federal Funds rate before and after 2008 financial crisis. 4-week-ahead forecast

Table 3.8: Volatility Connectedness with FFR during 2008 Financial Crisis

To (<i>i</i>) / From (<i>j</i>)	FFR	SPX	FTSE	FCHI	N225	From ($C_{i \leftarrow \bullet}$)
FFR	8.91	34.32	23.83	25.16	7.77	18.22
SPX	11.01	34.34	20.33	24.34	9.99	13.13
FTSE	14.30	32.59	19.86	23.99	9.25	16.03
FCHI	12.45	33.03	20.64	24.78	9.09	15.04
N225	8.24	33.67	22.27	25.55	10.28	17.94
To ($C_{\bullet \leftarrow j}$)	9.20	26.72	17.41	19.81	7.22	80.36 (Total C^H)
Net ($C_{\bullet \leftarrow j}^{Net}$)	-9.02	13.59	1.38	4.77	-10.72	

Volatility Connectedness Table with Federal Funds rate before and after 2008 financial crisis. 4-week-ahead forecast

Volatility System

Next, we look at the results of the spillover effect in the volatility system during the 2008 financial crisis, which are shown in Tables 3.7 and 3.8.

Table 3.7 depicts the connectedness in the volatility system without including the Federal Funds rate. The total spillover index during the financial crisis is 74.46%, much greater than the value of 65.04% for the 20-year whole sample shown in Table 3.3. So we could say that global stock volatilities interact much more with each other during the 2008 financial crisis. The increase in the total spillover index results from the decrease in the value of the diagonal elements and the increase in the value of the off-diagonal elements compared with Table

3.3. However, what is interesting is that there is little change in the diagonal elements for the S&P 500 index, but a significant decrease in the values for other stock markets. As for the off-diagonal elements, the values in the first column (the SPX column) and in the 4th row (the N225 row) see a significant increase, while the values of other diagonal elements do not have much increase, and some of them even encounter a decrease, compared with Table 3.3. This result shows that the US stock market has a dominant impact on the global stock markets during the financial crisis, while the Japanese stock market is mostly influenced by other markets. Therefore, we could see a significant increase in the value of the "To spillover" (26.42% compared with 19.07%) and the "Net spillover" (10.51% compared with 3.73%) for the S&P 500 index during the financial crisis, and a decrease in the "Net spillover" for the Nikkei 225 index.

We next analyze the results in Table 3.8, which shows the spillover in the volatility system when we include the Federal Funds rate during the financial crisis. First, the total spillover index now is 80.36%, which is even greater than that in Table 3.7. This outcome results from a very low value of the diagonal element for the Federal Funds rate, only 8.91%, which means that during the financial crisis, the US monetary policy is greatly influenced by the global stock market volatility, and it could no longer be considered as an "independent" policy. Second, the pairwise directional spillover from global stock markets to the Federal Funds rate is considerable during the financial crisis, with the greatest spillover of 34.32% from the S&P 500 index and the lowest spillover of 7.77% from the Nikkei 225 index. While on the contrary, the pairwise directional spillover from the Federal Funds rate to global stock markets could not be neglected either, with the largest value of 14.30% to the FTSE 100 index and the smallest value of 8.34% to the Nikkei 225 index. However, the pairwise directional spillover values from the Federal Funds rate to the volatility of stock indices are still lower than the values in the opposite direction, except for the Nikkei 225 index. Thus the "Net spillover" index for the Federal Funds rate in the volatility system is still negative during the financial crisis. Finally, due to the non-negligible spillover effect from the Federal Funds rate, the corresponding values in Table (3.8) are somewhat lower

than those in Table (3.7). Whereas the “Net spillover” of the volatility for all stock indices increases due to the negative “Net spillover” of the Federal Funds rate.

In a word, there is a deeper degree of interaction between the Federal Funds rate and the global stock market in the volatility system during the 2008 financial crisis. The US stock market is more influential during this period, while the Japanese stock market is dominated by the global stock market and the US monetary policy.

3.4.5 Spillover after the COVID-19 Outbreak

Now we look at the spillover effect between global stock markets after the outbreak of the COVID-19 pandemic. We believe that this pandemic started spreading worldwide beginning in March 2020, so we pick observations from Mar. 1, 2020, to Feb. 18, 2022, with a total of 102 observations after the outbreak of COVID.

Return System

The results of the spillover effect in the return system after the outbreak of COVID are shown in Table 3.9 and Table 3.10, with and without including the Federal Funds rate in our model, respectively.

Table 3.9 shows the spillover of the return system without the Federal Funds rate. First, the total spillover effect index is only 62.58%, slightly greater than the 20-year average value of 61.36% for the whole sample. It is quite interesting because the result is not consistent with what we show in Fig. 3.4, which indicates a greater total spillover after the outbreak of COVID. The reason is that for the rolling window analysis, the length of the window is 150 observations, while here we only have 102 observations after March 2020. Thus if we look at the periods before and after the sudden outbreak of COVID, the total spillover should be very high. However, now when we look at the period only after the outbreak of COVID, the stock markets seem more independent. Compared with Table 3.5, the values of the diagonal elements are greater, especially for the S&P 500 index (41.34% compared with 31.87%). Secondly, the value of the

off-diagonal elements of the first row and first column (the SPX row and column) is significantly lower than the values in Table 3.5. It indicates that the S&P 500 index is more independent after the COVID-19 outbreak than during the financial crisis, and its interaction with other markets has decreased since then. Finally, we could also see a decrease in the “To spillover” of the S&P 500 index, which results in a negative net information contribution to the return system.

Then we look at the results of the return system when we include the Federal Funds rate, which is summarized in Table 3.10. First, the total spillover index sees a large decrease compared with Table 3.9 (51.62% vs. 62.58), and it is due to the very high independence of the Federal Funds rate from the return system ($C_{FFR \leftarrow FFR}^H = 90.69\%$). Second, when we look at the pairwise directional spillover between the Federal Funds rate and the global stock markets, the global stock market does not have a significant impact on the Federal funds rate, which again explains the independence of the Federal Funds rate. On the other hand, except for the S&P 500 index, the pairwise directional spillover from the Federal Funds rate to stock markets is greater than that in the opposite direction, especially for the FTSE 100 index (10.53% vs. 0.26%). As a result, the Federal Funds rate has a net information contribution to the return system. Moreover, the corresponding values in Table 3.10 are close to those in Table 3.9, except for the elements in the third row and third column (the FTSE row and column) due to the considerable spillover from the Federal Funds rate to the FTSE 100 index, which causes a negative “Net spillover” for the FTSE 100 index.

Volatility System

The results of the spillover effect in the volatility system after the outbreak of COVID are shown in Table 3.11 and Table 3.12, without and with including the Federal Funds rate in our model, respectively.

Table 3.11 shows the spillover of the volatility system without the Federal Funds rate. First, the total spillover effect index is also very high, close to the value of Table 3.7 during the financial crisis (73.67% vs. 74.46%). Second, the values of the diagonal elements are close to each other,

Table 3.9: Return Connectedness without FFR after COVID Outbreak

To (<i>i</i>) / From (<i>j</i>)	SPX	FTSE	FCHI	N225	From ($C_{i \leftarrow \bullet}$)
SPX	41.34	20.32	21.05	17.29	14.66
FTSE	17.12	35.47	29.07	18.34	16.13
FCHI	16.79	28.29	34.27	20.66	16.43
N225	17.16	20.47	23.78	38.58	15.35
To ($C_{\bullet \leftarrow j}$)	12.77	17.27	18.47	14.07	62.58 (Total C^H)
Net ($C_{\bullet \leftarrow j}^{Net}$)	-1.89	1.14	2.04	-1.28	

Return Connectedness Table without Federal Funds rate after Mar 1, 2020. 4-week-ahead forecast

Table 3.10: Return Connectedness with FFR after COVID Outbreak

To (<i>i</i>) / From (<i>j</i>)	FFR	SPX	FTSE	FCHI	N225	From ($C_{i \leftarrow \bullet}$)
FFR	90.69	5.34	0.26	1.68	2.03	1.86
SPX	2.01	42.28	17.07	22.24	16.40	11.54
FTSE	10.53	12.96	33.02	24.22	19.26	13.40
FCHI	5.04	18.11	20.77	36.48	19.60	12.70
N225	2.76	17.29	18.70	21.83	39.42	12.12
To ($C_{\bullet \leftarrow j}$)	4.07	10.74	11.36	13.99	11.46	51.62 (Total C^H)
Net ($C_{\bullet \leftarrow j}^{Net}$)	2.21	-0.80	-2.04	1.29	-0.66	

Return Connectedness Table with Federal Funds rate after Mar 1, 2020.

with a minimum value of 24.94% for the CAC 40 index to a maximum value of 27.14% for the FTSE 100 index. Third, the values of the off-diagonal elements are also close to each other, which means that none of the stock markets have a significant net pairwise spillover to another one. And finally, the “Net spillover” of all the stock indices are close to zero (though not equal to zero). And the result indicates that there is no dominant stock market after the outbreak of COVID.

Then we look at the results of the volatility system after including the Federal Funds rate in our model which is summarized in Table 3.12. First, we notice a significant decrease in the total spillover index (57.56% vs. 73.67%), which is quite different from the result during the 2008 financial crisis, and this value is even lower than the 20-year average value of 62.73% for

the whole sample. The value of the diagonal element of the Federal Funds rate is not large, only 41.83%. However, we could see an increase in the values of all diagonal items of the volatility system, which indicates that each stock market becomes more independent from each others when we include the Federal Funds rate in the volatility system. This result is in contrast to the result of the period during the 2008 financial crisis. Next, we look at the off-diagonal elements of Table 3.12. We notice a considerable pairwise directional spillover from the stock markets to the Federal Funds rate (except for the Nikkei 225 index), as well as a non-negligible spillover in the opposite direction. Thus the interaction between the Federal Funds rate and the global stock market could not be ignored after the outbreak of COVID. However, for the rest of the off-diagonal elements, we could see a significant decrease compared with Table 3.11. Therefore, the seemingly high interaction in the volatility between global stock markets described in Table 3.11 lies in the spillover transmission effect of the Federal Funds rate, i.e., all the stock markets are to some extent correlated with the Federal Funds rate and this makes them seem to be correlated with each other. As a result, when we include the Federal Funds rate in the volatility system, we could see the true (or pure) interaction between the stock market decreases and each stock index becomes more independent from the system, especially the Nikkei 225 index.

The utterly contrary results of the spillover effect in the volatility system between the periods of the 2008 financial crisis and the wake of the outbreak of COVID suggest opposite global market trends after these two economic events. We see a deeper extent of globalization during the 2008 financial crisis, as the total spillover index is even higher after we include the Federal Funds rate in the volatility system. Whereas we notice a “de-globalization” trend in the wake of the outbreak of COVID since the stock indices become more independent from the volatility system, especially for the Japanese stock market (or the Asian stock markets).

Table 3.11: Volatility Connectedness without FFR after COVID Outbreak

To (<i>i</i>) / From (<i>j</i>)	SPX	FTSE	FCHI	N225	From ($C_{i \leftarrow \bullet}$)
SPX	26.83	26.27	24.11	22.79	18.29
FTSE	25.74	27.14	24.25	22.88	18.22
FCHI	26.34	26.58	24.94	22.14	18.76
N225	25.20	25.31	23.10	26.40	18.40
To ($C_{\bullet \leftarrow j}$)	19.32	19.54	17.86	16.95	73.67 (Total C^H)
Net ($C_{\bullet \leftarrow j}^{Net}$)	1.03	1.32	-0.90	-1.45	

Volatility Connectedness Table without Federal Funds rate after Mar 1, 2020. 4-week-ahead forecast

Table 3.12: Volatility Connectedness with FFR after COVID Outbreak

To (<i>i</i>) / From (<i>j</i>)	FFR	SPX	FTSE	FCHI	N225	From ($C_{i \leftarrow \bullet}$)
FFR	41.83	25.73	14.21	13.74	4.49	11.63
SPX	8.86	33.96	22.76	23.92	10.49	13.21
FTSE	8.48	15.07	41.63	22.62	12.20	11.67
FCHI	9.35	23.04	25.64	35.61	6.36	12.88
N225	4.62	9.07	17.18	9.94	59.19	8.16
To ($C_{\bullet \leftarrow j}$)	6.26	14.58	15.96	14.04	6.71	57.56 (Total C^H)
Net ($C_{\bullet \leftarrow j}^{Net}$)	-5.37	1.37	4.29	1.16	-1.45	

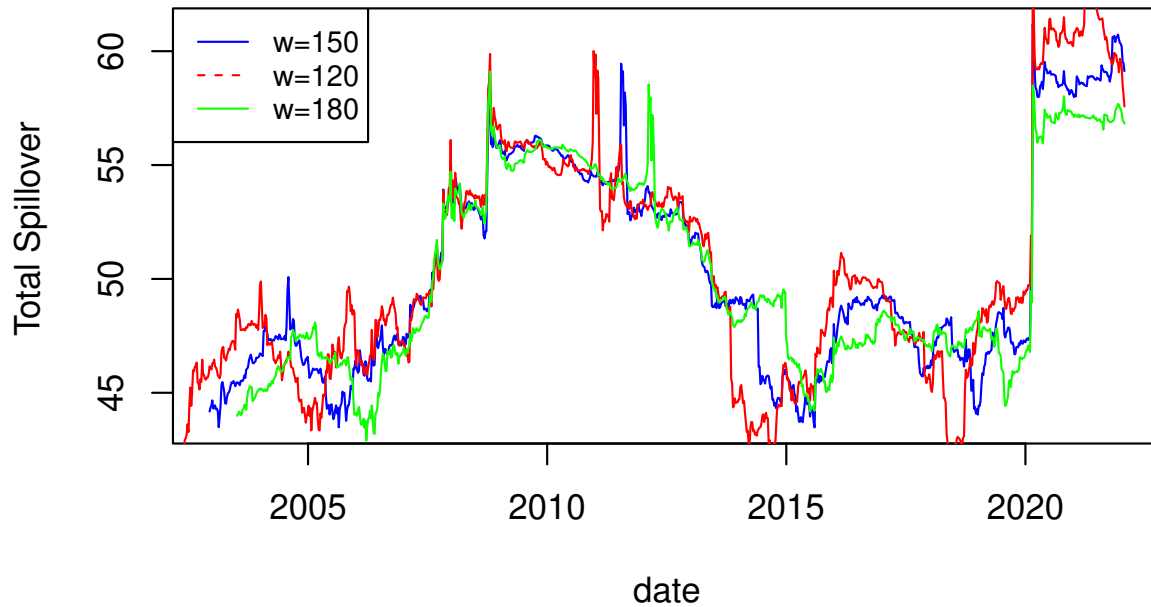
Volatility Connectedness Table with Federal Funds rate after Mar 1, 2020.

3.5 Robustness Test

In order to verify the robustness of our empirical results, we investigate the impact of the window length used in the estimation of the VAR model, including the Federal Funds rate. We choose $w = 150$ as the basic rolling window for our empirical analysis. Now we consider $w = 120$ and $w = 180$ as the rolling windows and compare the total spillovers of the two systems between different rolling window lengths. Fig. 3.8 and 3.9 show the total spillover for different rolling window lengths of the return system and the volatility system, respectively. The various rolling window total spillover results indicate that the dynamic pattern of the connectedness network does not vary much between different rolling window bases, and thus our empirical

results remain stable and are not influenced by the length of the window.

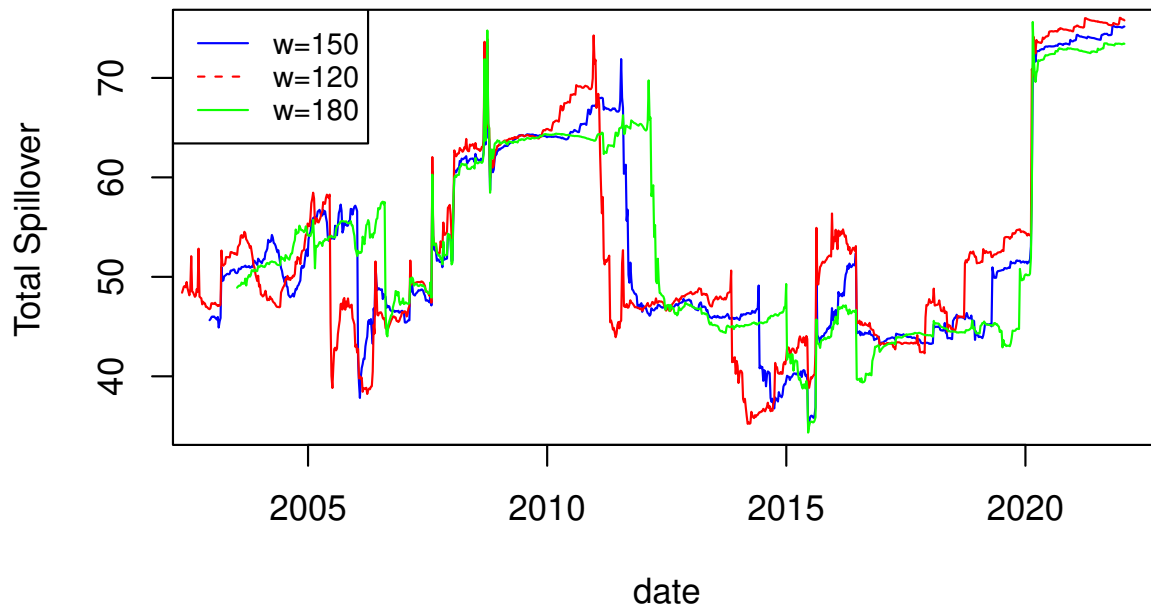
Figure 3.8: Dynamic Total Spillovers for Various Rolling Windows in the Return System



3.6 Conclusion

We apply an endogenous shock, the US monetary policy shock to the connectedness framework introduced by Diebold and Yilmaz (2009) and Diebold and Yilmaz (2012), to examine the interaction between the policy and global stock markets. With the introduction of the policy variable, we do find some differences in the spillover effect between global financial markets during the two financial crises - the 2008 financial crisis and the outbreak of COVID-19. What is more interesting is that since the causalities of the two crises are different, the results of our analysis also go in opposite directions for those two periods. The result of the 2008 financial

Figure 3.9: Dynamic Total Spillovers for Various Rolling Windows in the Volatility System



crisis suggests that the global stock markets are more connected during the crisis, while it indicates that the stock markets becomes more independent after the outbreak of COVID, which indicates the different trends of economic globalization for the two periods.

Here we use four stock indices to represent the global stock markets. In a further study, we could add the stock markets in more countries (like Canada, Australia, Stockholm, etc.) to the framework to see if the above results still hold. We can also use a different endogenous shock variable to examine the influence of the shock.

REFERENCES

- Abuzayed, B., Bouri, E., Al-Fayoumi, N., and Jalkh, N. (2021). Systemic risk spillover across global and country stock markets during the covid-19 pandemic. *Economic Analysis and Policy*, 71:180–197.
- Aït-Sahalia, Y., Mykland, P. A., and Zhang, L. (2005). How often to sample a continuous-time process in the presence of market microstructure noise. *Review of Financial Studies*, 18(2):351–416.
- Akhtaruzzaman, M., Boubaker, S., and Sensoy, A. (2021). Financial contagion during covid–19 crisis. *Finance Research Letters*, 38:101604.
- Andersen, T. (1994). Stochastic autoregressive volatility: A framework for volatility modeling. *Mathematical Finance*, 4:75–102.
- Andersen, T. G., Bollerslev, T., Diebold, F. X., and Labys, P. (2001). The distribution of realized exchange rate volatility. *Journal of the American Statistical Association*, 96(453):42–55.
- Anderson, T. G. and Bollerslev, T. (1998). Towards a unified framework for high and low frequency return volatility modeling. *Statistica Neerlandica*, 52(3):273–302.
- Anderson, T. G., Bollerslev, T., Diebold, F. X., and Labys, P. (2003). Modeling and forecasting realized volatility. *Econometrica*, 71(2):579–625.
- Antonakakis, N., Chatziantoniou, I., and Filis, G. (2017). Energy consumption, co2 emissions, and economic growth: An ethical dilemma. *Renewable and Sustainable Energy Reviews*, 68:808–824.
- Arif, M., Hasan, M., Alawi, S. M., and Naeem, M. A. (2021). Covid-19 and time-frequency connectedness between green and conventional financial markets. *Global Finance Journal*, 49:100650.
- Bandi, F. M. and Russell, J. R. (2006). Separating microstructure noise from volatility. *Journal of Financial Economics*, 79(3):655–692.
- Barndorff-Nielsen, O. E., Hansen, P. R., Lunde, A., and Shephard, N. (2009). Realized kernels in practice: trades and quotes. *The Econometrics Journal*, 12(3):1–32.
- Barndorff-Nielsen, O. E. and Shephard, N. (2002). Econometric Analysis of Realized Volatility and its Use in Estimating Stochastic Volatility Models. *Journal of the Royal Statistical Society Series B: Statistical Methodology*, 64(2):253–280.
- Bollerslev, T. (1986). Generalized autoregressive conditional heteroskedasticity. *Journal of Econometrics*, 31(3):307–327.
- Bouri, E., Cepni, O., Gabauer, D., and Gupta, R. (2021). Return connectedness across asset classes around the covid-19 outbreak. *International Review of Financial Analysis*, 73:101646.

- Carr, P. and Wu, L. (2006). a tail of two indices. *Journal of Derivatives*, 13(3):13–29.
- Christoffersen, P., Feunou, B., Jacobs, K., and Meddahi, N. (2014). The economic value of realized volatility: Using high-frequency returns for option valuation. *Journal of Financial and Quantitative Analysis*, 49:663–697.
- Corsi, F., Mittnik, S., Pigorsch, C., and Pigorsch, U. (2008). The volatility of realized volatility. *Econometric Reviews*, 27(1-3):46–78.
- Diebold, F. X. and Mariano, R. S. (1995). Comparing predictive accuracy. *Journal of Business & Economic Statistics*, (3):253–263.
- Diebold, F. X. and Yilmaz, K. (2009). Measuring financial asset return and volatility spillovers, with application to global equity markets. *the Economic Journal*, 119(534):158–171.
- Diebold, F. X. and Yilmaz, K. (2012). Better to give than to receive: Predictive directional measurement of volatility spillovers. *International Journal of Forecasting*, 28(1):57–66.
- Diebold, F. X. and Yilmaz, K. (2014). On the network topology of variance decompositions: Measuring the connectedness of financial firms. *Journal of Econometrics*, 182(1):119–134.
- Ehrmann, M. and Fratzscher, M. (2009). Global financial transmission of monetary policy shocks. *Oxford Bulletin of Economics and Statistics*, 71(6):739–759.
- Engle, R. F. (2002). New frontiers of arch models. *Journal of Applied Econometrics*, 17(5):425–446.
- Engle, R. F. (2004). Risk and volatility: Econometric models and financial practice. *American Economic Review*, 96(3):405–420.
- Engle, R. F. and Gallo, G. M. (2006). A multiple indicators model for volatility using intra-daily data. *Journal of Econometrics*, 131(1):3–27.
- Engle, R. F. and Ng, V. K. (1993). Measuring and testing the impact of news on volatility. *The Journal of Finance*, 48(5):1749–1778.
- Errunza, V. R. and Losq, E. (1985). The behavior of stock prices on ldc markets. *Journal of Banking & Finance*, 9(4):561–575.
- Eun, C. S. and Shim, S. (1989). International transmission of stock market movements. *The Journal of Financial and Quantitative Analysis*, 24(2):241–256.
- Forsberg, L. and T, B. (2002). Bridging the gap between the distribution of realized (ecu) volatility and arch modeling (of the euro): the garch-nig model. *Journal of Applied Econometrics*, 17(5):535–548.
- Gerlach, R., Naimoli, A., and Storti, G. (2020). Time-varying parameters realized garch models for tracking attenuation bias in volatility dynamics. *Quantitative Finance*, 20(11):1849–1878.
- Glosten, L. R., Jagannathan, R., and Runkle, D. E. (1993). On the relation between the expected value and the volatility of the nominal excess return on stocks. *The Journal of Finance*, 48(5):1779–1801.

- Hahm, S.-M. (2004). Transmission of stock returns and volatility: The case of Korea. *the Journal of the Korean Economy*, 5(1):17–45.
- Hancock, G. D. (2012). Vix and vix futures pricing algorithms: Cultivating understanding. *Modern Economy*, 3:284–294.
- Hansen, P. R. and Huang, Z. (2016). Exponential garch modeling with realized measures of volatility. *Journal of Business Economics Statistics*, 34(2):269–287.
- Hansen, P. R., Huang, Z., and Shek, H. H. (2011). Realized garch: A joint model for returns and realized measures of volatility. *Journal of Applied Econometrics*, 27(6):877–906.
- Hansen, P. R., Huang, Z., Tong, C., and Wang, T. (2022). Realized garch, cboe vix, and the volatility risk premium. *Journal of Financial Econometrics*, pages 1–37.
- Hansen, P. R. and Lunde, A. (2006). Realized variance and market microstructure noise. *Journal of Business Economic Statistics*, 24(2):127–161.
- Hao, J. and Zhang, J. E. (2013). Garch option pricing models, the cboe vix, and variance risk premium. *Journal of Financial Econometrics*, 11:556–580.
- Hilliard, J. E. (1979). The relationship between equity indices on world exchanges. *The Journal of Finance*, 34(1):103–114.
- Huang, Z., Wang, T., and Hansen, P. R. (2020). *Realized GARCH, the CBOE VIX, and the volatility risk premium*, page Working paper.
- Jeon, B. N. and Furstenberg, G. M. V. (1990). Growing international co-movement in stock price indexes. *Quarterly Review of Economics and Business*, 30(3):15–31.
- Kambouroudis, D. S. and McMillan, D. G. (2016). Does vix or volume improve garch volatility forecasts? *Applied Economics*, (13):1210–1228.
- Kanniainen, J., Lin, B., and Yang, H. (2014). Estimating and using garch models with vix data for option valuation. *Journal of Banking Finance*, pages 200–211.
- Kim, S. (2001). International transmission of u.s. monetary policy shocks: Evidence from var's. *Journal of Monetary Economics*, 48(2):339–372.
- Kloek, T. and van Dijk, H. K. (1978). Bayesian estimates of equation system parameters: An application of integration by monte carlo. *Econometrica*, 46(1):1–19.
- Kundu, S. and Sarkar, N. (2016). Return and volatility interdependences in up and down markets across developed and emerging countries. *Research in International Business and Finance*, 36:297–311.
- Laeven, L. and Tong, H. (2012). Us monetary shocks and global stock prices. *Journal of Financial Intermediation*, 21(3):530–547.

- Liesenfeld, R. and Richard, J. F. (2006). Classical and bayesian analysis of univariate and multivariate stochastic volatility models. *Econometric Reviews*, 25(2-3):335–360.
- Liu, C. (2016). Spillover effects in major equity markets: A garch bekk approach. *Open Access Library Journal*, 3:1–21.
- Liu, Y. A. and Pan, M.-S. (1997). Mean and volatility spillover effects in the u.s. and pacific-basin stock markets. *Multinational Finance Journal*, 1(1):47–62.
- Luo, R., Zhang, W., Xu, X., and Wang, J. (2018). A neural stochastic volatility model. *Proceedings of the AAAI Conference on Artificial Intelligence*, 32(1).
- Malliaris, A. G. and Urrutia, J. L. (1992). The international crash of october 1987: Causality tests. *The Journal of Financial and Quantitative Analysis*, 27(3):353–364.
- Mathur, I. and Subrahmanyam, V. (1990). Interdependencies among the nordic and u.s. stock markets. *The Scandinavian Journal of Economics*, 92(4):587–597.
- Meddahi, N. (2002). A theoretical comparison between integrated and realized volatility. *Journal of Econometrics*, 17(5):479–508.
- Miranda-Agrippino, S. and Rey, H. (2020). U.S. Monetary Policy and the Global Financial Cycle. *The Review of Economic Studies*, 87(6):2754–2776.
- Miyakoshi, T. (2003). Spillovers of stock return volatility to asian equity markets from japan and the us. *Journal of International Financial Markets, Institutions and Money*, 13(4):383–399.
- Moon, G.-H. and Yu, W.-C. (2010). Volatility spillovers between the us and china stock markets: Structural break test with symmetric and asymmetric garch approaches. *Global Economic Review*, 39(2):129–149.
- Nelson, D. B. (1991). Conditional heteroskedasticity in asset returns: A new approach. *Econometrica*, 59(2):347–370.
- Nishimura, Y. and Men, M. (2010). The paradox of china's international stock market comovement: Evidence from volatility spillover effects between china and g5 stock markets. *Journal of Chinese Economic and Foreign Trade Studies*, 3(3):235–253.
- Noureldin D, Shephard, N. and Sheppard, K. (2012). Multivariate high-frequency-based volatility (heavy) models. *Journal of Applied Econometrics*, 27(6):907–933.
- Panda, A. K., Nanda, S., and Paital, R. R. (2019). An empirical analysis of stock market interdependence and volatility spillover in the stock markets of africa and middle east region. *African Journal of Economic and Management Studies*, 10(3):314–335.
- Panton, D. B., Lessig, B. P., and Joy, O. M. (1976). Comovement of international equity markets: A taxonomic approach. *The Journal of Financial and Quantitative Analysis*, 11(3):415–432.
- Pesaran, H. H. and Shin, Y. (1998). Generalized impulse response analysis in linear multivariate models. *Economics Letters*, 58(1):17–29.

- Richard, J.-F. and Zhang, W. (2007). Efficient high-dimensional importance sampling. *Journal of Econometrics*, 141(2):1385–1411.
- Ripley, D. M. (1973). Systematic elements in the linkage of national stock market indices. *The Review of Economics and Statistics*, 55(3):356–361.
- Robichek, A. A., Cohn, R. A., and Pringle, J. J. (1972). Returns on alternative investment media and implications for portfolio construction. *The Journal of Business*, 45(3):427–443.
- Saeed, T., Bouri, E., and Alsulami, H. (2021). Extreme return connectedness and its determinants between clean/green and dirty energy investments. *Energy Economics*, 96:105017.
- Schwert, G. W. (1989). Why does stock market volatility change over time? *the Journal of Finance*, 44(5):1115–1153.
- Shephard, N. and Sheppard, K. (2010). Realising the future: forecasting with high-frequency-based volatility (heavy) models. *Journal of Applied Econometrics*, 25(2):197–231.
- Simons, D. P. (2003). The nasdaq volatility index during and after the bubble. *Journal of Derivatives*, 11(2):9–24.
- So, M. E. P., Lam, K., and Li, W. K. (1998). A stochastic volatility model with markov switching. *Journal of Business & Economic Statistics*, 16(2):244–253.
- Song, Y., Ji, Q., Du, Y.-J., and Geng, J.-B. (2019). The dynamic dependence of fossil energy, investor sentiment and renewable energy stock markets. *Energy Economics*, 84:104564.
- Stein, E. M. and Stein, J. C. (1991). Stock Price Distributions with Stochastic Volatility: An Analytic Approach. *The Review of Financial Studies*, 4(4):727–752.
- Taylor, S. J. (2007). *Modelling Financial Time Series (SECOND EDITION)*. World Scientific Publishing.
- Wang, T., Liang, F., Huang, Z., and Yan, H. (2022). Do realized higher moments have information content? - var forecasting based on the realized garch-rsrk model. *Economic Modelling*, page 105781.
- Youssef, M., Mokni, K., and Ajmi, A. N. (2021). Dynamic connectedness between stock markets in the presence of the covid-19 pandemic: does economic policy uncertainty matter? *Financial Innovation*, 7(13).
- Zakoian, J.-M. (1994). Threshold heteroskedastic models. *Journal of Economic Dynamics and Control*, 18(5):931–955.
- Zhang, W. and Hamori, S. (2021). Crude oil market and stock markets during the covid-19 pandemic: Evidence from the us, japan, and germany. *International Review of Financial Analysis*, 74:101702.

APPENDICES

APPENDIX

A

TABLES AND FIGURES

Description of statistics of the stock indices in Chapter 1.

Table A.1: Descriptive statistics for daily returns

stock index	T	Min	Median	Mean	Max	SD	Kurtosis	Skewness
SPX	1000	-12.67	0.1201	0.0601	8.961	1.334	21.32	-1.086
FTSE	1000	-10.14	0.0282	-0.0008	7.782	1.149	14.46	-0.9139
STOXX50E	1000	-12.01	0.0558	0.0180	8.655	1.258	17.23	-1.065
N225	1000	-6.274	0.0745	0.0362	7.731	1.233	7.614	-0.1619
OMXSPI	1000	-11.81	0.1248	0.0555	7.014	1.156	17.48	-1.440
STI	1000	-8.363	-0.0052	-0.0047	6.000	0.983	14.61	-0.6786

Table A.2: Descriptive statistics for 5-min realized volatility

stock index	T	Min	Median	Mean	Max	SD	Kurtosis	Skewness
SPX	1000	0.0122	0.3271	0.9629	41.53	2.949	99.31	8.943
FTSE	1000	0.0133	0.4763	1.140	66.68	3.277	188.4	11.61
STOXX50E	1000	<0.0001	0.5101	1.145	46.72	3.263	100.2	9.163
N225	1000	0.0206	0.3409	0.6700	38.49	1.692	271.7	13.89
OMXSPI	1000	0.0401	0.3364	0.5803	20.55	1.260	126.6	9.914
STI	1000	0.0720	0.2738	0.4027	12.16	0.6843	130.5	9.819

Figure A.1: The Daily Returns of 6 Stock Indices

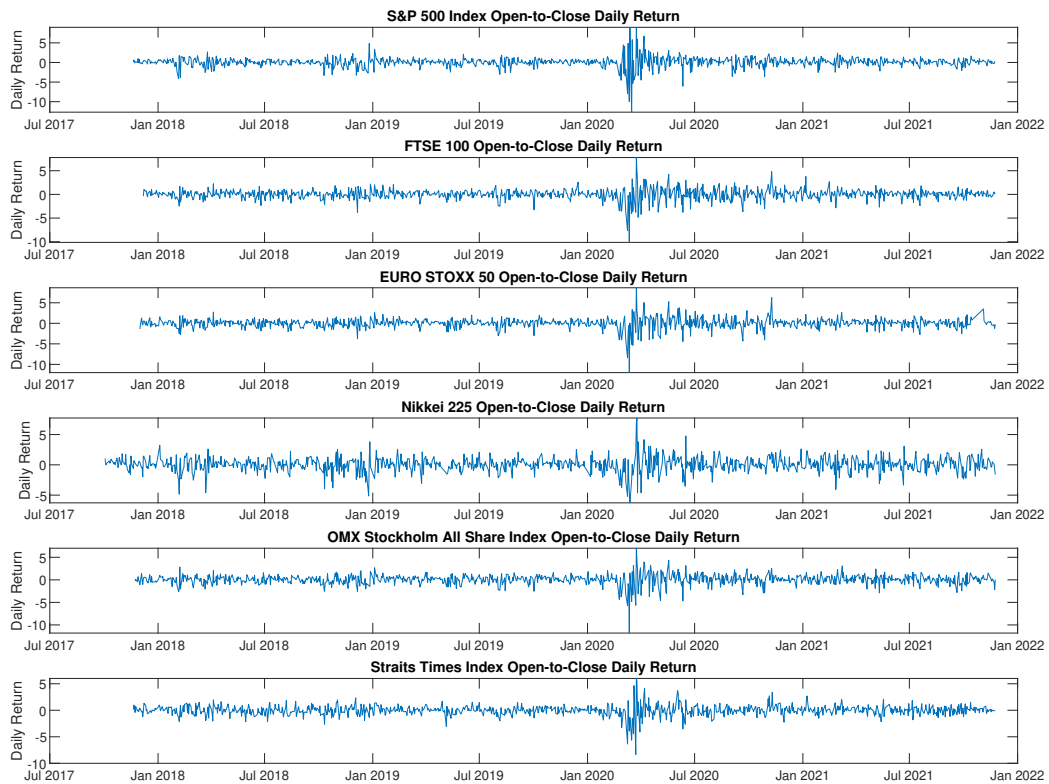
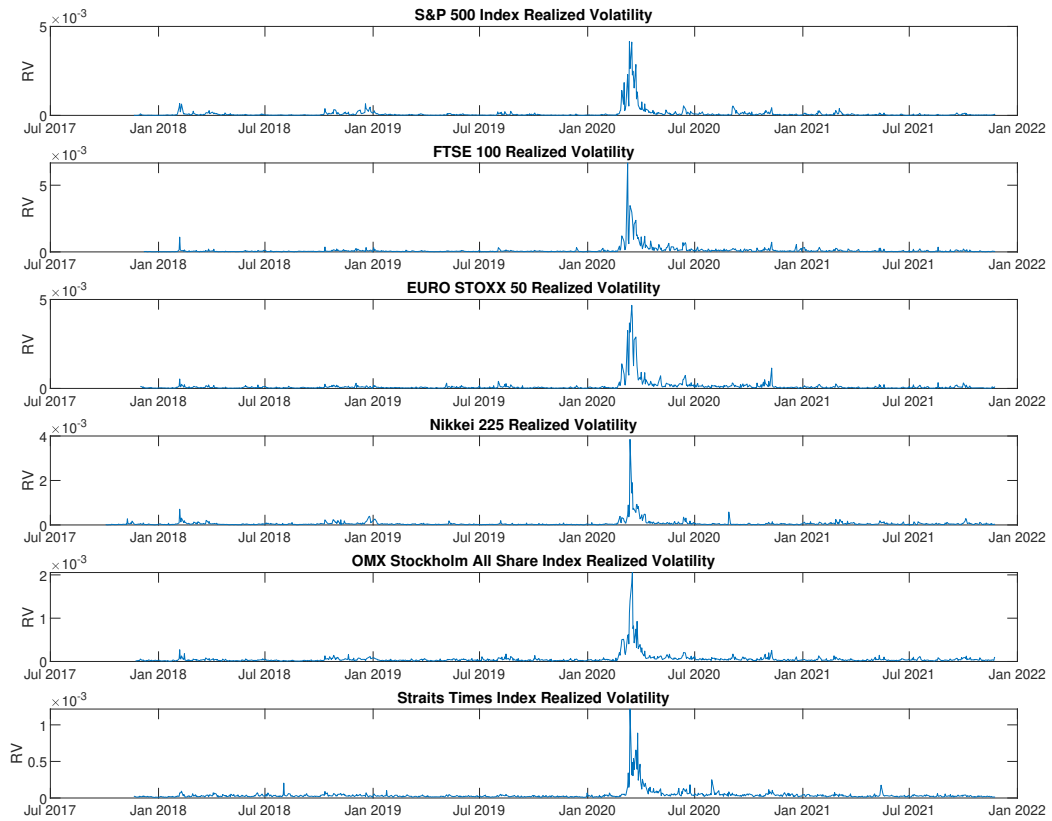


Figure A.2: The 5-Min Realized Volatility of 6 Stock Indices



APPENDIX

B

CALCULATION OF VIX

The algorithm used in calculating the VIX from the S&P 500 index options is based on the work of Carr and Wu (2006) and Hancock (2012). To begin the calculation, we first identify the variances of the out-of-the-money options for the near-term (σ_1^2) and the next-term (σ_2^2) contract months:

$$\sigma_1^2 = \frac{2}{T_1} \sum_{i=1}^n \frac{\Delta X_{1,i}}{X_{1,i}^2} Q(X_{1,i}) e^{r_1 T_1} - \frac{1}{T_1} \left(\frac{F_1}{X_{1,0}} - 1 \right)^2 \quad (\text{B.1})$$

$$\sigma_2^2 = \frac{2}{T_2} \sum_{i=1}^n \frac{\Delta X_{2,i}}{X_{2,i}^2} Q(X_{2,i}) e^{r_2 T_2} - \frac{1}{T_2} \left(\frac{F_2}{X_{2,0}} - 1 \right)^2 \quad (\text{B.2})$$

where T_1 and T_2 are the number of minutes to the maturity for the near-term and next-term contracts, respectively, as a proportion of the number of minutes in a year, F_1 and F_2 is the forward index level derived from index option prices shown in Eq. (B.3), $X_{1,i}$ and $X_{2,i}$ are the

strike prices of the i th out-of-money option, $Q(X_{1,i})$ and $Q(X_{2,i})$ denotes the mid-quote price for each out-of-money option at strike $X_{1,i}$ and $X_{2,i}$, $X_{1,0}$ and $X_{2,0}$ are the first strikes below the forward index level F_1 and F_2 , r_1 and r_2 are the coupon-equivalent yields on the T-bill maturing closest to expiration, and $\Delta X_{1,i}$ and $\Delta X_{2,i}$ denotes the interval between strike prices shown in Eq. (B.4). The near-term contract is the contract which will expire soon.

$$F_j = X_{j,0} + (C_{j,0} - P_{j,0})e^{r_j T_j}, \quad j = 1, 2 \quad (\text{B.3})$$

$$\Delta X_{j,i} = \frac{X_{j,i+1} - X_{j,i}}{2}, \quad j = 1, 2 \quad (\text{B.4})$$

Then, the COBE linearly interpolates between the two variances of near-term and next-term contracts to obtain a variance of 30-day maturity. The VIX is the annualized percentage of the 30-day variance, defined as:

$$VIX = 100 \sqrt{\left[T_1 \sigma_1^2 \frac{N_{T_2} - N_{30}}{N_{T_2} - N_{T_1}} + T_2 \sigma_2^2 \frac{30 - N_{T_1}}{N_{T_2} - N_{T_1}} \right] * \frac{365}{30}} \quad (\text{B.5})$$

where N_{T_1} and N_{T_2} denotes the number of minutes until settlement of the near-term and next-term options, respectively.

APPENDIX

C

DIEBOLD-MARIANO TEST

Diebold and Mariano (1995) propose a method, which is later called the Diebold-Mariano test, to compare the forecasting performance of different models. Here we use this method to test the MSE difference between our model and the benchmark model.

Let $d_t = \hat{e}_{1t}^2 - \hat{e}_{2t}^2$, where $\{\hat{e}_{1t}\}_{t=1}^T$ denotes the losses of the Realized GARCH-VIX model (the difference between the predicted value and true value), and $\{\hat{e}_{2t}\}_{t=1}^T$ represents the losses of the benchmark Realized GARCH model. Then we call the $\{d_t\}_{t=1}^T$ as a loss-differential series. If the loss-differential series is stationary and short memory, then we have the asymptotic distribution of the sample mean of loss differential:

$$\sqrt{T}(\bar{d} - \mu) \xrightarrow{d} N(0, 2\pi f_d(0)),$$

where

$$\bar{d} = \frac{1}{T} \sum_{t=1}^T (\hat{e}_{1t}^2 - \hat{e}_{2t}^2)$$

is equal to the MSE difference divided by T ,

$$f_d(0) = \frac{1}{2\pi} \sum_{t=-\infty}^{\infty} \gamma_d(\tau)$$

is the spectral density of the loss differential at frequency 0,

$$\gamma_d(\tau) = E[(d_t - \mu)(d_{t-\tau} - \mu)]$$

is the autocovariance of the loss differential at displacement τ , and μ is the expectation of the loss differential. Then the statistic to test the null hypothesis of equal forecast accuracy is

$$DM = \frac{\bar{d}}{\sqrt{\frac{2\pi \hat{f}_d(0)}{T}}}$$

where $\hat{f}_d(0)$ is a consistent estimate of $f_d(0)$, and DM follows student-t distribution.

We could obtain a consistent estimate of $2\pi f_d(0)$ by taking a weighted sum of the available sample autocovariances

$$2\pi \hat{f}_d(0) = \sum_{\tau=-(T-1)}^{T-1} I\left(\frac{\tau}{M}\right) \hat{\gamma}_d(\tau)$$

where

$$\hat{\gamma}_d(\tau) = \frac{1}{T} \sum_{t=|\tau|+1}^T (d_t - \bar{d})(d_{t-|\tau|} - \bar{d})$$

and $I(\tau/M)$ is the lag window, M is the truncation lag. We could use the rectangular truncation window, defined by:

$$I\left(\frac{\tau}{M}\right) = \begin{cases} 1, & \text{for } |\frac{\tau}{M}| \leq 1 \\ 0, & \text{otherwise} \end{cases}$$

In practice, we could use the truncation lag $M = T^{1/3}$.